Numerical Study

of

Effervescent Atomization

SEYED MILAD MOUSAVI

A Thesis

In

The Department of

Mechanical and Industrial Engineering

Presented in Partial Fulfillment of the Requirements

for the Degree of Master of Applied Science (Mechanical Engineering) at

Concordia University

Montreal, Quebec, Canada

January 2014

Concordia University

Numerical study of Effervescent atomization

Abstract

Atomization is a process where the bulk of liquid jet disintegrates into liquid sheets, ligaments and droplets. It has enormous applications in industries and processes such as combustion, heat transfer systems, transport, biological systems and particularly our interest, coating processes. The Effervescent nozzle is a type of twin-fluid atomizer and has shown a superior performance in handling and spraying different liquids without any clogging issues; which is particularly interesting in thermal spray. In spite of significant number of experimental works, a few numerical works have been carried out. That makes it crucial to conduct a comprehensive numerical study on Effervescent atomizer.

The complex internal and external behaviors of Effervescent atomizer are governing the behavior of the flow. The latter is a turbulent and compressible multiphase flow. It is studied numerically by employing a three-dimensional compressible Eulerian method along with Volume of Fluid (VOF) surface-tracking method coupled with the Large Eddy Simulation (LES) turbulence model. The numerical study is conducted by using OpenFoam library, an open-source package introduced by Open-CFD.

In this study, the effect of varying the gas to liquid ratio (GLR) and the suspension (i.e. effect of viscosity, density and surface tension), on the structure of internal flow and consequently, the external flow is studied numerically. It is observed that the increase in GLR is accompanied with an evolution of the internal flow from a complex bubbly flow to an annular flow. This reduces the liquid film thickness at the discharge orifice. Further studies on internal pressure illustrated the critical condition,

choked flow and pressure oscillations at the discharge orifice. The examination of increasing the GLR and evolving of internal flow resulted in changing in primary atomization parameters such as shortening the breakup length and widening the spray cone angle. Furthermore, the existence of a slip velocity between the two phases in the external flow results in dominant aerodynamic forces at high GLRs. Moreover, alternation of the liquid properties illustrated the higher spray velocity and wider cone angle of the spray, which demonstrates the superior performance of the Effervescent atomizer.

Acknowledgments

I would like to express sincere thanks to my supervisor Dr. Ali Dolatabadi for his great supports and encouragements through entire program of my master degree. His great advices and constant guidance during my studies were always helpful. I also I would like to express my thanks to NSERC for financially supporting this project.

I also would like to appreciate all the great support of my beloved family, especially my mother, and father who are always my symbols. I am speechless about the efforts that they did for me to achieve my goals.

Finally, I thank all of my friends in thermal spray group, Navid Sharifi, Maniya Aghaibeig, Fadhel ben ettouil as well as my friend in CFD lab, Mehdi jadidi, Hamed Farshchi Tabrizi and Matin komeili, Dennis de Pauw and all others whose names are missing for their great help. I also would like to thank Hany Gomaa for his great help.

Seyed Milad Mousavi

Table of contents

List of Figures

List of tables

Nomenclatures

Letters

c_v	Specific heat
Co	Courant number
D_O	Orifice diameter
D_g	Gas core diameter
e	Average internal energy
F_b	Body force
g	Gravity
k	Kinetic energy
l	Length
n	Interface unit normal vector
p, P	Pressure
q	Heat flux
Q	Volumetric flow rate
R	Gas constant
S	Surface area vector
t	Time
T	Temperature
U	Velocity
U_r	Relative normal velocity of interface

Greek Letters

ρ	Density
α	Liquid volume fraction
ε	Energy dissipation
δ	Arbitrary small value
μ	Dynamic viscosity
ϑ	Kinematic viscosity
σ	Surface tension
κ	Curvature
ψ	Compressibility factor
τ	Stress tensor

Abbreviations

SPS	Suspension Plasma Spraying
HVSFS	High Velocity Suspension Flame Spraying
HVOF	High Velocity Oxygen Fuel

GLR	Gas to liquid ratio
SMD	Sauter Mean Diameter
MAC	Marker and Cell
VOF	Volume of Fluid
LS	Level set
SGS	Subgrid scale
LES	Large Eddy Simulation

Subscripts

g	gas
l	liquid
ml	Molecular
$Turb$	Turbulent
SGS	Subgrid scale

1 Motivation and background

In this chapter, an introduction on the multiphase flow and the motivations of this study are briefly discussed. The atomization process and various atomizers are introduced. In addition, "Effervescent nozzle" and its effective parameters are described in details. Finally, the outline of thesis and its objectives are summarized.

1.1   Introduction and motivation

Multiphase flow is one of the most important topics in engineering systems, especially regarding the optimization of their operating conditions. The multiphase phenomenon is not just limited to industrial technology. Instead, it can be observed in wide range of applications, from natural to biological applications, which need more in depth understanding. Few of the important industrial fields that multiphase flow understanding is important are power systems, combustion, coating processes, heat transfer systems, transport, lubrication, biological systems, and environmental control systems.

Obviously, the above applications have different behaviors and characteristics, which are very interesting to researchers in order to analyze the particular systems' problems.   However, the general studies of thermo-fluid dynamics for the multiphase flow have not yet been developed as much as it is for the single-phase flow. In order to predict the behavior of these systems accurately, complicated mathematical models are required.

Two-phase flow can be classified according to the mixture phases or the structure of the interface. By neglecting the plasma phase, multiphase flow can be classified into four different types. First the Gas-Solid mixture, second the Gas-liquid mixture, third the Liquid-solid mixture and finally the Immiscible-liquid mixture. It is important to note that although the last group is not typically a two-phase; its behavior can be analyzed by considering it as a two-phase mixture [1].

Coating processes and techniques are one of the fields in which various multiphase flows, as well as other thermo physical and physical processes, are combined.

A detailed investigation, on each of those processes is required, due to their high complexity. The processes that are currently used to produce metallic or nonmetallic coatings are generically called Thermal spray. The working principle for different categories of Thermal spray is to have heated particles transformed into molten or semimolten materials, and then they are accelerated and propelled toward the substrate due to high kinetic energy of the process gases. Those categories can be summarized as flame spray; electric arc spray, plasma arc spray, and recent cold spray technique, which is a relatively low temperature process. The high velocity and high temperature, in few of those methods, particles plastically deform upon the impact and form a bounding with the substrate, which results in a layer of coating on it [2]. Schematic of typical thermal spray process is shown in   Fig. 1-1 [3].

Thermal spray processes are generally categorized in three or recently four major categories. For example, Flame spray, Electrical arc spray, Plasma spray and recently, Cold spray. There are differences between the temperature and kinetic energy of each of these methods that will be briefly discussed in the following session. Determinant parameters for the selection of thermal spray technique are the coating materials, economical aspects, and the efficiency of the coating as well as the portability of the equipment [2].
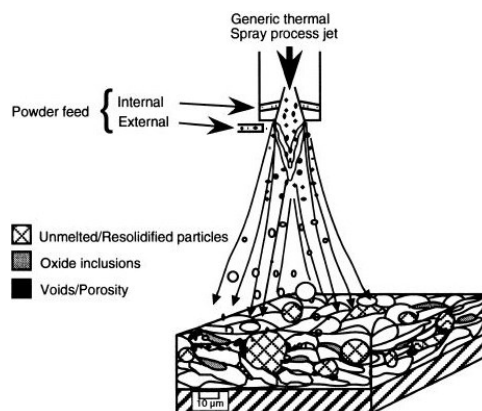
Figure 1-1 Schematic of a typical thermal spray process [3]

In Conventional coating processes, particles dispersed in carrier gas, are injected into a high velocity and in few cases in a high temperature gas. However, this method of injection has few drawbacks in the new emerging thermal sprays techniques, where tendency of coating of submicron and nano sized particles is increasing. In such a context, the drawbacks of conventional injection methods cause troubles in the submicron and nano particles injection. Those issues are due to the agglomeration and injector clogging issues as well as the tendency of particles to follow the flow streamlines. This results in divergence of particles and consequently preventing the impingement of fine particles on the substrate [4].

The best-known suggested method for fortifying these issues is the injection of solid particles through suspensions [5]. Accordingly, the suspension of solid particles is obtained by suspending the solid particles in the base fluid such as water or ethanol. Profiting from suspension spray technique leads to the obtaining of unique surface properties such as robust wear resistance, superior catalytic behavior for electrodes, used in fuel cells [6], enhanced thermal insulation as well as producing superhydrophobic surfaces [7].

The first step in Suspension Plasma Spraying (SPS) and High Velocity Suspension Flame Spraying (HVSFS) is to obtain a stable suspension by using different techniques such as adding surfactant or increasing viscosity. These methods prevent particles from agglomeration and consequently sedimentation. The second step is the injecting of suspension into flame/jet, as shown in Fig. 1-2 [8]. Through this process, suspension is primarily atomized to droplets, subsequently the liquid phase of the

suspension evaporates, the remaining particles absorb heat, then they are transformed into molten or semimolten particles and finally they impinge on the substrate. Suspension penetration along with the primary and secondary atomizations of the suspension intensively affect the final coating quality [9, 10]. For instance, the higher the suspension momentum, the more intense cooling occurring in jet/flame. Hence, the particles might not be molten. In contrast, if the momentum flux of the suspension could not reach to the appropriate amount, particles cannot become molten or semimolten due to the lack of penetration of the suspension jet [11].

(a)   (b)
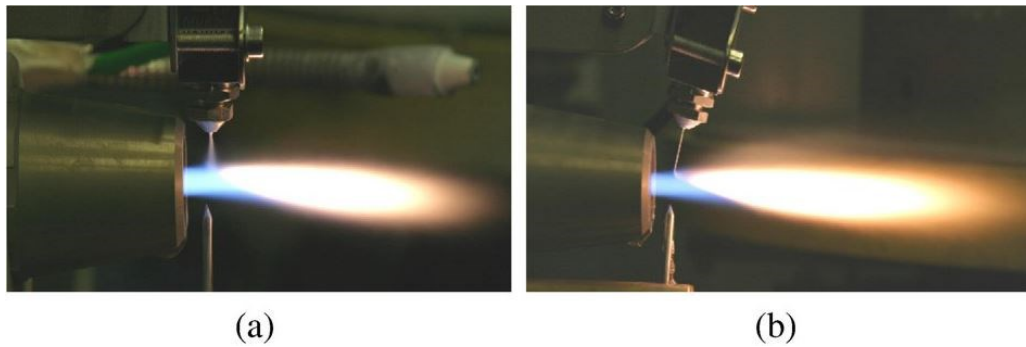
Figure 1-2 Suspension injection: a) spray injection and b) liquid jet injection [8]

According to the discussed phenomena occurring in thermal spray, the significant effect of atomization is obvious in the suspension coating processes. This motivates researchers to investigate the different methods of the atomization to obtain better quality coatings.

1.2   Atomization

Following the mentioned industrial applications of atomization, the transformation of liquid jet into small droplets and sprays is required. According to industrial process requirements, different kinds of spraying devices have been developed. For instance, in combustion processes, disintegration of liquid jet into droplets increases surface area of the fuel in contact with hot gas. The enhanced surface area results in a more efficient, better and cleaner combustion. In other applications such as thermal spray coatings, jet or aerated-liquid of suspension is injected into plasma plume or High Velocity Oxygen Fuel (HVOF) in order to coat a surface of a substrate by semi-molten or molten particles that are remaining from evaporation of the liquid phase of the suspension.

Although various applications have been mentioned, the main phenomena occurring through these devices are fundamentally similar. Generally, the hydraulic behavior of fluid inside nozzles determines the degree of turbulence of the flow. The small disturbances inside the nozzle propagate through the interface of liquid. Consequently, it disintegrates a jet of liquid into the sheets, then ligaments and droplets. In fully turbulent flows, when the jet exits the orifice, the only parameter bounding radial component of velocity is the surface tension. By overcoming surface tension forces, the jet disintegrates into the liquid sheets, ligaments, and subsequently the droplets. However, the mechanism of disintegration of the liquid sheets with or without perforation varies. In perforated liquid sheets, holes tend to coalescence, which results in the disintegration of sheets. In contrast, in liquid sheets without perforation, waves are produced on liquid sheets due to interactions between gas and liquid phases and leads to

fragmentation of the liquid sheet. The mechanism governing the phenomena is called the wavy-sheet disintegration.

The factors influencing atomization performance can be categorized into two different groups. The first is related to the geometrical design of the atomizer that results in various nozzles. Each nozzle has dependency on its design parameters, where the most important parameter is the diameter of discharge orifice. The second factor is physical properties of the dispersed phase (operating liquid) and continues phase (ambient condition). According to each specific design of the atomizers and operating conditions, internal flow characteristics evolve. This is due to the flow separation, cavitation, turbulence vortex, or two-phase flow happening inside nozzle, which leads to various spray characteristics. For clarifying the effective factors on atomization, it is initially required to understand multiphase flow regimes. Classification of two-phase flows, while considering the interface structure, was reported by Ishii [1], Table 1-1. He reviewed the work of Wallis (1969), Hewitt and Hall Taylor (1970), Collier (1972), Govier and Aziz (1972), Zuber (1971), Ishii (1971) and Kocamustafaogullari (1971). Classification according to the structure of flow interface results in three different multiphase classes subdivided to three or four subclasses. The three main categories are Separated flow, Mixed or Transitional flow and finally Dispersed flow.

Table 1-1 Two phase flow classification (Ishii, [1])

Class	Typical regimes	Geometry	Configuration	Examples
Separated flows	Film flow		Liquid film in gas Gas film in liquid	Film condensation
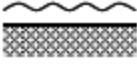
7

				Film boiling
	Annular flow		Liquid core and gas film Gas core and liquid film	Film boiling Boilers
	Jet flow		Liquid jet in gas Gas jet in liquid	Atomization Jet condenser
Mixed or Transitional flows	Cap, Slug or churn-turbulent flow		Gas pocket in liquid	Sodium boiling in forced convection
	Bubbly annular flow		Gas bubbles in liquid film with gas core	Evaporators with wall nucleation
	Droplet annular flow		Gas core with droplets and liquid film	Steam generator
	Bubbly droplet annular flow		Gas core with droplets and liquid film with gas bubbles	Boiling nuclear reactor channel
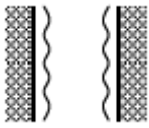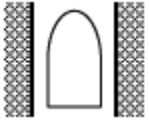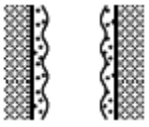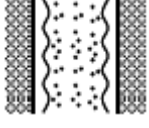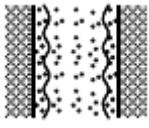
Dispersed flows	Bubbly flow		Gas bubbles in liquid	Chemical reactors
	Droplet flow		Liquid droplets in gas	Spray cooling
	Particulate flow		Solid particles in gas or liquid	Transportation of powder
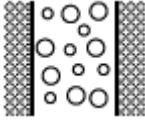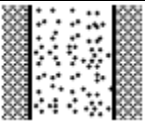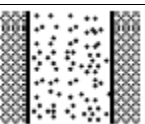
Depending on how the structure of interface is, the separated flow can be subdivided to three more sub groups. Additionally, these divisions can be done for mixed or transitional flow as well as dispersed flows. Each of them is separated to four and three subgroups, respectively. Some of these different flow types are shown in Fig. 1-3.
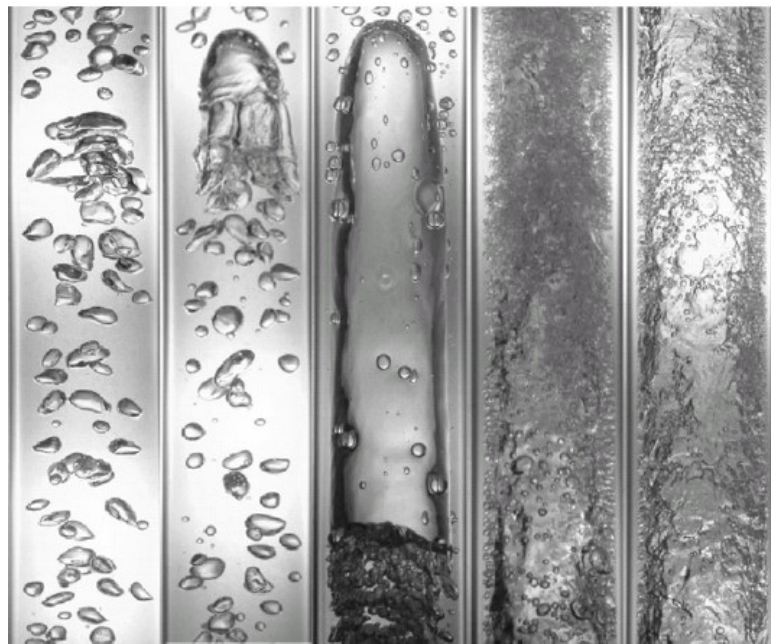
Figure 1-3 Air-water flow in a vertical 25.4 mm diameter pipe [1] Left to right: bubbly flow, bubbly slug flow, slug flow, droplet annular flow, annular flow

1.3   Atomizers

As mentioned above, different types of atomizers have been developed. Generally, each atomizer produces high relative velocity between the surrounding gas and the liquid which facilitates the atomization. These various atomizers have been categorized based on their geometry and working conditions. The most common atomizers used in industry include Pressure, Rotary, Air-assist, Air-blast, Twin-fluid, Electrostatic, Ultrasonic, Whistle, and Effervescent atomizers.

Pressure atomizers working principle is based upon the conversion of high-pressure to high kinetic energy. This occurs while the liquid is passing through the discharge orifice. Plain orifice, Pressure swirls, Square spray, Duplex dual orifice, Spill return and Fan spray are included in Pressure atomizers. The common advantages of pressure atomizers are simplicity in design and good atomization. However, the dual orifice is considered as an exception as it suffers from complexity in its design. The main drawbacks of all these atomizers are that they require high-pressure supply. In addition, a few of them suffer from clogging issues, and narrow range of spray cone or variation in cone angle based on the inlet flow rate. Moreover, they are highly sensitive to the liquid properties, which alter all spray characteristics in those atomizers.

In the rotary atomizers depicted in Fig. 1-4 [12, 13], a high speed rotating disk, or cup, forces the liquid outward leading to fragmentation of liquid into droplet in low mass flow rates and into liquid sheets and ligaments in higher flow rates close to periphery edge. In some cases, especially for lower mass flow rates, the rotating disk includes holes or guide vanes for producing better atomization. One of the immense advantages of rotary atomizers is independency of rotational speed of disk and flow rate that gives a

flexibility in various operating conditions. Moreover, they are capable of atomizing the slurries without any clogging issues, whereas 360-Degrees atomization pattern narrows down their applications. This makes them particularly not applicable in thermal spray.
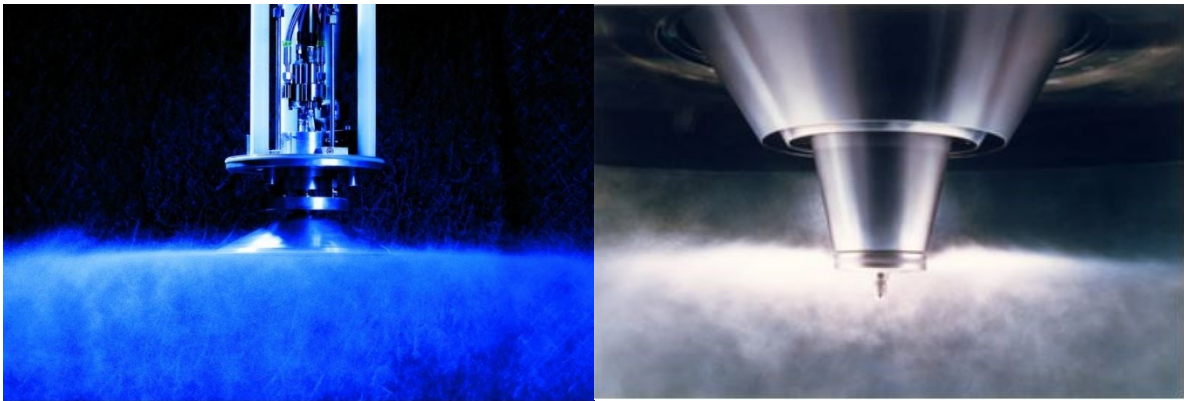
Figure 1-4 Rotary atomizer [12, 13]

Twin-fluid atomizer is a category of atomizers where two types of fluids are interacting to produce atomization. Their immense benefits are their low injection pressure and low flow rate that are required to produce fine droplets. Since low injection pressure of gas stream along with fine atomization forms an attractive combination, they became more popular in many industrial applications such as combustion, coatings processes, spray drying, etc. Air-blast and Air-assist atomizers fundamentally fall into the same category while there are some differences in the amount and velocity of air being exposed to the liquid. The small amount of air, with high velocity, is exposed to the liquid internally or externally. This is based on the design of Air-Assist atomizers, which include internal-mixing and external-mixing configurations. Although external-mixing configuration does not have a backpressure issue, that results in backflow of fluid into air vanes, it is less energy efficient than internal-mixing. However, energy inefficiency is a main drawback for both. On the other hand, in Air-Blast atomizers, a good atomization is

obtained by employing larger amount of gas with lower velocity. Plain jet and Prefilming are two types of such atomizers. Although Plain jet is cheaper and simpler, Prefilming shows superior atomization performance even in high ambient pressure, which makes it one of the best choices for gas turbines. For additional information regarding other types of atomizers, "Atomization and Spray" by Lefebvre [14] could be beneficial.

In addition to the above atomizers, "Effervescent nozzle" is a distinct type of atomizer falling into the internal-mixing twin-fluid category of atomizers. However, the principal technique contrarily differs from other type of atomizers in this category. At the outset, this technique was introduced by Lefebvre et al. [15, 16, 17] and Roesler [18] as "aerated liquid atomization" in early 1990s. The term "Effervescent atomization" was primarily used by Buckner et al. [19, 20]. The principal of Effervescent nozzle is explained in details in the following sections.

1.4   Effervescent atomization

1.4.1 Effervescent nozzle in the literature

In contrast to other types of twin-fluid atomizers, the technique of Effervescent atomization is based on the injection of small amounts of low pressure gas into the bulk of the liquid through aerator holes. This forms a bubbly or annular two-phase flow depending on the amount of injected gas in the mixing chamber. The mixture of multiphase flow goes through an exit orifice and consequently atomization will occur [21]. Based on the method of gas injection into the liquid, Effervescent atomizers are divided into two different configurations. Those are the inside-out and the outside-in Effervescent atomizers. A typical inside-out configuration of effervescent nozzle is

depicted in Fig. 1-5 [22]. As illustrated, it is made from the following parts: Liquid inlet, Air Inlet, aerator tube and holes, mixing –chamber, and the discharge orifice.
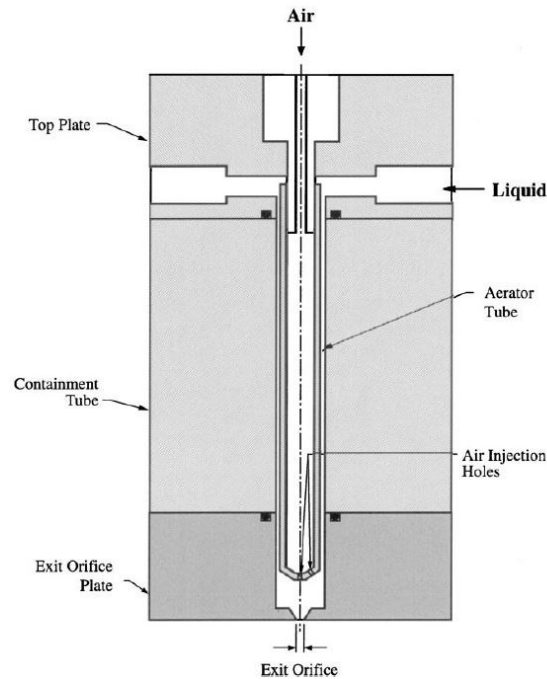
Figure 1-5 Inside-out configuration of the Effervescent nozzle [22]

In this configuration, in contrast to the outside-in configuration, a small amount of atomizing gas is injected into the mixing chamber and it forms various flow regimes from bubbly to annular flow depending on the amount of injected gas. The bubbles trapped in liquid phase burst upon exiting the discharge orifice due to pressure jump occurring in exit orifice. This scatters the bulk of liquid into the liquid sheets, ligament and consequently droplets [23]. The mixing process and the geometry of nozzle will affect the multiphase flow behavior inside the mixing chamber and therefore the atomization [17].

During the past two decades, researches revealed the advantages of the Effervescent nozzle in comparison to the conventional, Twin-Fluid and Rotary atomizers. Previously illustrated experimental results show that the pressure required for good atomization is much lower than what is needed for other types of atomizers [16, 17, 19].

In such context, the Drop sizes for each specific pressure are smaller than what is obtained by other conventional methods [16, 18, 19]. Moreover, due to lower inject pressure; the gas flow rate is much lower than other kinds of twin-fluid atomizers. Consequently, less energy is required to inject atomizing gas [16, 18, 19]. Furthermore, the diameter of the discharge orifice is greater than conventional nozzles' exit diameters, accordingly they have a higher flow rate and lower probability of clogging [18, 24]. In addition to other benefits of using Effervescent nozzle, it is particularly beneficial in combustion applications. This is due to its ability to reduce the pollutant emissions because of the existence of air in the spray core [16]. The effect of viscosity of liquid on the mean drop size is relatively low, which shows the capability of Effervescent nozzle to handle different liquids [25, 26]. It should be added that due to the lower exit velocity of the fluid, than those for conventional nozzles, erosion is decreased for injecting suspension by an Effervescent nozzle [27].

As the effervescent nozzle has characteristics of twin fluid nozzle, its efficiency is higher than pressure or rotary atomizers in respect to the amount of energy required for atomization. Chawla [27] has investigated the speed of sound in multiphase and single-phase flow and revealed that the better atomization performance of twin fluid nozzle with respect to single fluid is due to the difference of speed of sound in the single phase and the two-phase flow. For example, he demonstrated that the speed of sound in the water/air mixture is in the range of 20 to 30 m/s. On the other hand, this is changed to 300 and 1500 m/s for each of the fluids, water or air, respectively. Because of the lower sonic speed, the fluid would choke at lower velocities, which creates greater pressure jump even in low exit velocity. This helps the nozzle to have a better atomization.

14

Moreover, having a choked flow through an orifice has the advantage that larger orifice can be used [22]. Roesler and Lefebvre [18] visually investigated the principals of the flow inside the nozzle. They reported that the inside bubbly flow may transform towards the orifice exit to either bubbly or slug flow. In the bubbly flow, rapid expansion of flow at orifice exit causes the atomization whereas in slug flow, the air inside the jet causes atomization, which are illustrated schematically in Fig. 1-7. This kind of atomization is the key point of effervescent nozzle.
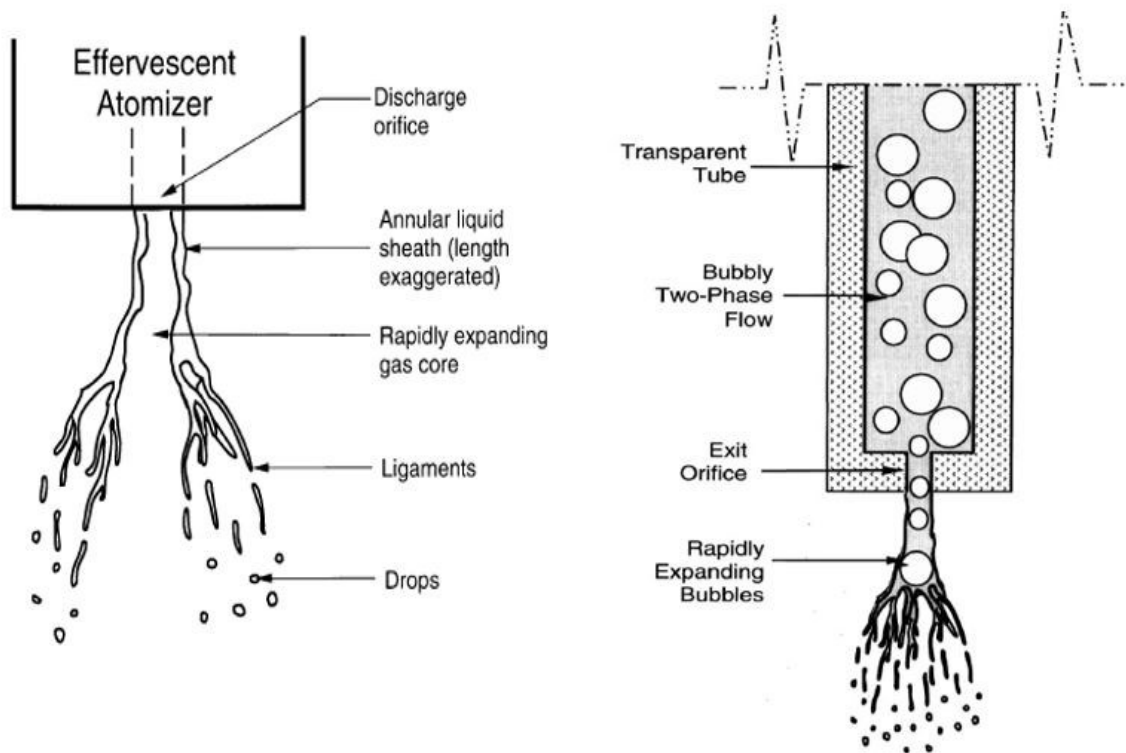
Figure 1-6 Atomization of the annular flow observed by Sojka et al. [20] and atomization mechanism for the bubbly flow observed by Roesler and Lefebvre [18]

The independent parameters affecting the spray characteristics of Effervescent nozzle are categorized by Sovani et al. [22], Table 1-2, which includes injection pressure

drop, Gas to liquid ratio (GLR), physical properties of liquid and internal geometry of the nozzle.

Table 1-2 Geometrical variables affecting spray characteristics [22]

Independent variable	description
Outside-in/inside-out gas injection	The method of injecting gas into the liquid which is sometimes from inside or outside of liquid
Size, number and location of aerator holes	Effect on bubble size and bubble evolution inside nozzle
Mixing chamber size, shape and relative position correspond to final exit orifice	Effect on internal evolution of two phase flow
Contraction contour at orifice inlet	Effective on flow regime change inside orifice
Length and diameter of exit orifice	Indicates the atomizer flow rate and drop size
Profile of orifice exit	Change the spray characteristics
Number of exit orifice	Shows different characteristics for non-homogenous flows

The effect of physical properties of the liquid, such as viscosity and surface tension has been investigated by different researchers. However, it should be noted that these properties of fluid could not be studied separately and these properties act as a

package. Few researchers like Buckner and Sojka [25, 26] reported that the viscosity of liquid has no effect on droplet mean diameter. Nevertheless, Lund et al. [28] and Sutherland et al. [29, 30] indicated a small dependency of droplet mean diameter to viscosity. Lund et al. [28] illustrated that a four times increase in viscosity results in only 15% increase in droplet mean diameter. In contrast to these results, which were obtain in lower injection pressure in the range of 0.2-2.0 MPa, Satapathy [31] demonstrated strong dependency of mean droplet size to viscosity in relatively higher pressure range of 11-33 MPa .

In terms of surface tension effects, Lund et al. [28] and Sutherland et al. [29, 30] reported contrary results. Lund et al. [28] reported an increase in Sauter Mean Diameter (SMD) by growth of surface tension from 0.030 to 0.067 $\frac{kg}{s^2}$ while Sutherland et al.'s [29, 30] results indicated that SMD remains the same by varying the surface tension. Liu et al. [32] experimentally studied the effect of fluid physical properties on unsteadiness of Effervescent atomization for water and mixture of water/glycerol. They realized that the increase in GLR for water results in more unsteady spray while the outcomes for mixture indicate that spray is more unsteady by the reduction in GLR.

Lund et al. [33] also investigated the influence of gas phase molecular weight on the droplet size where they reported that deduction of the gas molecular weight leads to a small increase in the droplet mean diameter. Moreover, Rahman et al. [34] indicated weak dependency of droplet mean diameter to gas molecular weight where their results prove what Lund et al. [33] reported.

1.4.2 Fluid mechanics of effervescent nozzle

Spray characteristics are determined by independent variables, inside and outside of the atomizer, such as operating conditions, internal geometry and liquid physical properties. The dependent variables such as drop size and velocity of droplets are affected by the structure of internal flow. As there are many parameters affecting the internal flow as well as the external flow, the two-phase flow associated with effervescent atomizers is more complex than those for the conventional twin-fluids are.

Roesler and Lefebvre [18, 35] experimentally investigated the internal flow of an Effervescent nozzle. They carried out experiments on the effect of pressure and GLRs between 0.005 and 0.10 on the flow. Their photographical studies revealed that in low GLRs, single bubbles flow sequentially inside the jet and by rapid expansion at the orifice exit, atomization occurres. By deducing GLR, bubbles start to coalesce, which evolves the bubbly flow regime to slug-flow regime along with few instabilities occurring. By further increase in GLRs, the flow changes to an annular flow.

On the other hand, another approach has been used by Chin and Lefebvre [36] to study the parameters of Effervescent nozzle. They corresponded the internal flow to two-phase flow inside horizontal and vertical pipes. Their studies lead to certain conclusion. First, the range of GLRs for maintaining the bubbly flow can be increased by deducing the injection pressure and same as for vertical flows. Second, the flow has gradual transition from bubbly flow to slug and annular flow by increasing the GLRs. In addition, their work demonstrated that the viscosity increase could maintain bubbly flow in the mixing chamber whereas the surface tension influence is opposite to viscosity but considerably smaller.

Whitlow and Lefebvre [37] visually studied the transition of bubbly flow to slug flow in a more detailed manner, while being able to precisely define the transition point. They tested the nozzle with pressure range between 0.069 and 0.69 MPa and GLRs between zero and 0.06. In low pressure the transition from bubbly flow to slug flow occurred suddenly, which helped in the determination of the transition point. However, gradual transition for higher pressure makes this determination more subjective. By assuming a one-dimensional steady flow, the maximum GLR attained while the flow remains in bubbly regime, was formulated by Whitlow and Lefebvre and described in equation 1. Studies of the flow inside Effervescent nozzle remains too limited and mostly the external flow has been studied and modeled.

$$GLR_{max} = \left(\frac{\rho_g}{\rho_l}\right)\left(\frac{1}{\alpha_{max}-1}\right)^{-1} \tag{1}$$

Santangenlo and Sojka [38] studied empirically near nozzle structure of Effervescent spray. The external flow near the nozzle was visualized under a working pressure range lying between 0.1 and 1.1 MPa. The different regime structures depending on GLRs were noticed. In GLRs that are less than 0.02, a single gas bubble that is surrounded by liquid films is discharged from the orifice exit and then by its expansion and bursting, the atomization occurs. Annular flow regime occurs in GLRs that are higher than 0.05. This is because of the bubble coalescence, which makes a ring of ligaments around the gas after breaking up of annular ring.

In comparison to the large number of studies that have been experimentally carried out on Effervescent nozzle, few researchers have worked on the modeling of this

process. Even though they mostly focused on the external flow due to the complexity of the two-phase flow. Initially, Buckner and Sojka [39] proposed a model that is based on the mass flow rate of liquid, gas phase, and fluid properties to calculate the mean droplet size after primary breakup. It was improved by Lund et al. [28] by adding the effect of atomizer exit geometry. While Lund et al. [28] did not consider the aerodynamic effect of gas, Sutherland et al. [29] added the influence of relative velocity between gas phase and liquid phase. However, none of those researchers considered secondary atomization of droplets while Lin et al. [40] predicted the droplet mean size by introducing a 3-D model for primary and secondary atomization using Lagrangian approach. Despite the complexity of the phenomena occurring inside, which affects the flow outside of nozzle, a few researchers tried to simulate the internal flow. Esfarjani and Dolatabadi [41] three dimensionally simulated the structure of two-phase flow inside the Effervescent nozzle using incompressible Eulerian-Eulerian approach. They studied the effect of fluid properties on the thickness of liquid in discharge passage of orifice in different GLRs. They illustrated that the fluid properties do not have significant effect on the film thickness. Although their approach has few drawbacks, it should be noted that their work was the first simulation on Effervescent nozzle. They managed to understand few aspects of internal flow such as film thickness and the effect of viscosity and density by resembling the suspension without considering surface tension. As mentioned earlier, they employed Eulerian-Eulerian approach; nevertheless, they were forced to use averaging approach in order to calculate the film thickness. During their analysis, they did not employ any surface tracking method to capture the interface between the two phases. Thus, few fundamental phenomena such as evolution of the interface,

disturbances on the interface that are the source of atomization in primary atomization, surface tension effect and external flow are missing in their study.

In this study, which is a continuation of their work, a surface capturing method is employed and compressibility is considered to achieve a more comprehensive model on multiphase flow for Effervescent nozzle. Furthermore, as most of experimental setups are only able to quantitatively study the far field, there is lack of near field study. Therefore, in this study, in addition to investigation on the internal flow, near field external flow is investigated to obtain better understanding of the reason of far field characteristics. Available surface capturing method is briefly discussed in the next section.

1.5   Numerical methods for surface tracking

Although the effervescent nozzle has been experimentally studied well through the past two decades, only a few simulations for external flow and even less for internal flow have been carried out. For simulating the multiphase flow, various Eulerian, Lagrangian or a mixture of both approaches can be used. However as it has been shown in experimental studies, the phenomena that occur in an Effervescent nozzle is very complicated. The interface between the two phases is considered as a discontinuity in computational cells requiring a special treatment. In numerical simulation of these kinds of flows, complex deforming interface of liquid and gas should be accurately captured. These methods can be categorized according to the type of flow modeling, interface modeling, flow-interface coupling or the type of spatial discretization [42].

For Interface solving, there are two general diverse methods. One is using grids moving with the interface that is Lagrangian whereas the other is using fixed grid points,

which is mixed Lagrangian-Eulerian or pure Eulerian approach. In fixed grid method, another indicator required for capturing the interface. These methods are divided into three different groups depending on the type of indicator. First the interface capturing, second the interface tracking and finally the combined techniques. Examples of these categories for the first group are Marker and Cell (MAC) [43], Volume of fluid (VOF) [44], Level set (LS) [45] and defuse interface [46]. In addition, Glimm's front tracking method [47] as the second group and lastly the combined method such as Tryggvason's front tracking [48], sharp interface [49], immersed boundary [50] and immersed interface [51].

Annaland et al. [52] have outlined the advantages and disadvantages of some of these methods. Those are demonstrated in Table 1-3.

Table 1-3 Brief comparison of the different techniques [extracted from [52]]

Method	Advantages	Disadvantages
Front tracking	Extremely accurate	Mapping of interface mesh onto Eulerian mesh
	Robust	
	Account for substantial topology changes in interface	Dynamic remeshing required
		Merging and breakage of interfaces requires sub-grid model
	Merging and breakage of interfaces does not occur automatically	
Level set	Conceptually simple	Limited accuracy
	Easy to implement	Loss of mass (volume)
Shock capturing	Straightforward implementation	Numerical diffusion

	Abundance of advection schemes are available	Fine grids required Limited to small discontinuities
Marker particle	Extremely accurate Robust Accounts for substantial topology changes in interface	Computationally expensive Re-distribution of marker particles required
SLIC VOF	Conceptually simple Straightforward extension to three dimensions	Numerical diffusion Limited accuracy Merging and breakage of interfaces occurs automatically
PLIC VOF	Relatively simple Accurate Accounts for substantial topology changes in interface	Difficult to implement in three dimensions Merging and breakage of interfaces occurs automatically
Lattice Boltzmann	Accurate Accounts for substantial topology changes in interface	Difficult to implement Merging and breakage of interfaces occurs automatically

Considering our application, in spite of its high accuracy, the Front-tracking method cannot be used due to the lack of auto merging and breakage of the interfaces. Level set, Shock capturing and Marker particle method were not applicable in our case due to the lack of mass conservation in unrefined regions, limitation for small discontinuity, and computationally expensiveness for 3D cases, respectively for each method. The common

method that is extensively being employed in highly deforming interface is Piece Wise Linear Interface Construction Volume of Fluid (PLIC VOF). This method is suitable for the current study because of its advantages. Those are summarized as, the benefits gained from the auto merging and breakage of the interface, mass conservation as well as its accuracy. However, it should be mentioned that it suffers slightly from diffusion of interface.

1.6 Objective

The lack of numerical study of effervescent nozzle is the main motive to numerically study the internal and near-field external flows of Effervescent nozzle. In order to achieve such a goal, bubble evolution and consequently the flow in the discharge passage of orifice, together with their influence on external flow will be investigated. This is carried out by employing compressible two-phase model along with VOF method. Those are able to capture surface evolution and disturbances as well as pressure jump and choking phenomena, in addition to the external primary atomization of liquid phase. In this study, the effect of GLR is initially studied in the range between 0.55 to 2.5%. In addition, the effect of liquid properties will be studied. In terms of external flow, average velocity of droplets and ligaments along with cone angle of spray and breakup length will be compared in different cases. The objectives of this thesis can be summarized as the study of:

- The bubble evolution and internal flow inside the nozzle
- The liquid film thickness at the discharge orifice
- The phenomena happening in discharge passage of orifice

- The primary atomization of external flow and its characteristics such as velocity and cone angle

1.7 Thesis outline

In Chapter 2, the methodology of numerical study is presented in details. At the outset, the Compressible Volume of Fluid method is described along with discretization schemes, mesh generation, boundary conditions, and the employed solver. In Chapter 3, the results of numerical simulation for an effervescent nozzle are presented. The numerical results are validated according to the previous experimental work carried out in our group. In this chapter, the influence of Gas to Liquid Ratio (GLR) on the internal and external flow is presented and the characteristics of the external flows are studied. The parameters investigated are internal flow pattern, liquid film thickness, cone angle and breakup length, pressure and choking condition, average velocity of liquid and finally the effect of liquid properties. Chapter 4 consists of the work conclusions and the potential future works.

2 Methodology

In this chapter, the governing equations and the methodology of this study are briefly described. The boundary and initial conditions employed on this study are enlightened. Moreover, a brief description of the finite volume framework used in the simulation is included in this chapter.

2.1 Compressible Volume of Fluid Method

Following the clarification made in section (1.5), Compressible VOF method is employed for this study. The principal of the model is proposed by several researchers, therefore a brief outline of the model and governing equations are presented. It should be mentioned that all the simulation are carried out using Open Source Field Operation and Manipulation (OpenFOAM) C++ libraries, which is an opensource CFD toolbox developed by OpenCFD Ltd [53].

The governing equations for computational model for Compressible phenomena occurring in Effervescent nozzle are described by applying mixture continuity and momentum equations for compressible flows,

$$\frac{\partial \rho}{\partial t} + \nabla. \rho U = 0 \tag{2}$$

$$\frac{\partial \rho U}{\partial t} + \nabla. (\rho UU) = -\nabla p + \nabla. (\mu \nabla U) + (\nabla U). \nabla \mu - \rho g - g.x\nabla \rho + \sigma \kappa \nabla \alpha \tag{3}$$

where U is the velocity vector, modified pressure term $p^* = p - \rho g.x$, x is coordinate vector, ρ is the density, σ is the surface tension and k is the curvature of interface. The distribution and weighted average mixture density and viscosity of fluid are calculated using α which is volume fraction of the main phase.

$$\rho = \alpha \rho_l + (1 - \alpha) \rho_g \tag{4}$$

$$\mu = \alpha \mu_l + (1 - \alpha) \mu_g \tag{5}$$

where g and l are the subscripts indicating liquid and gas phases, respectively. In VOF method of OpenFOAM a scalar indicator, here α, is defined in order to designate the interface. The values of α based on the Heaviside function is unity in liquid phase, zero in gas phase and a distribution between zero and unity for the interface between both. The function of this scalar indicator is as follows,

$$
\alpha = \begin{cases} 1 & \text{in liquid} \\ 0 < \alpha < 1 & \text{at the interface} \\ 0 & \text{in gas} \end{cases} \tag{6}
$$

If the value of α is between zero and one, it indicates a point at two-phase interface. The α function values are schematically shown in Fig. 2-1.

0	0	0	0	0
0	0	0.15	0.7	0.9
0	0.01	0.8	1	1
0	0.3	1	1	1
0	0.45	1	1	1

Figure 2-1 Schematic Distribution of volume

fraction for a typical case

In numerical solution of high-density ratio flows, significant errors in calculation of physical properties could occur as a result of small errors in calculation of volume fraction. Hence, it is essential to calculate the volume fraction accurately for the assessment of surface curvature required for the determination of surface tension forces and pressure gradient on the free surface. As the VOF method is mesh dependent, the

accuracy of interface reconstruction is entirely related to mesh resolution. According to the following equation, the discontinuity will spread into the computational domain.

$$\frac{\partial \alpha}{\partial t} + (V.\nabla)\alpha = 0 \qquad (7)$$

The finite volume scheme is employed to discretize the governing equations. Furthermore, Rusche [54] proposed a bounded compression term, which leads to a sharper interface between the different phases. The modified equation of volume fraction with extra artificial compressive term is as follows,

$$\frac{\partial \alpha}{\partial t} + (V.\nabla)\alpha + \nabla.\left(U_r \alpha(1 - \alpha)\right) = 0 \qquad (8)$$

where U_r is a relative normal velocity of interface and is equal to,

$$U_r = k_c n \max \frac{|n.U|}{|S|^2} \qquad (9)$$

$$n = \frac{\nabla \alpha}{|\nabla \alpha| + \delta} \qquad (10)$$

where n, the interface unit normal vector, is calculated by obtaining the gradient of α at the cell faces, δ is a small amount to avoid singularity where $\nabla \alpha = 0$, S is the surface area vector and k_c is an adjustable coefficient to define the amount of compression in equation 8, chosen to be $k_c = 2$ in this study. This is done in order to achieve sharper interface. Furthermore, the artificial compression term helps to achieve sharper interface without affecting the solution outside the region due to $\alpha(1 - \alpha)$ term, which automatically diminishes the effect of compressive term outside of the interface. This

modified method promotes a sharper interface capturing in comparison to classical VOF method. In addition, due to the sort of discretization used for convective term of Eq. 8, numerical diffusion is unavoidable, even though it can be minimized by benefiting from discretization of compressive term, subsequently capturing sharper interface. The surface tension that affects only interfacial cells modeled as body force using the Continuum Surface Force method [54].

$$F_b = \sigma k \nabla \alpha \tag{11}$$

where the curvature of free surface, k, is defined by,

$$k = -\nabla.\left(\frac{\nabla \alpha}{|\nabla \alpha|}\right) \tag{12}$$

The energy equation is solved to obtain the compressibility factor,

$$\frac{\partial \rho e}{\partial t} + \nabla.(\rho U e) - \nabla.q + p\nabla.U = 0 \tag{13}$$

where q represents the summation of molecular and turbulent heat flux and e is the average of internal energy based on volume fraction,

$$q = q_{ml} + q_{Turb} \tag{14}$$

$$e = \frac{c_{v,l}\alpha_l\rho_l T + c_{v,g}(1-\alpha_l)\rho_g T}{\rho} \tag{15}$$

Since the equation of state is essential for closure of the chosen system of equations in compressible flow, ideal gas law is employed to calculate compressibility of gas phase as shown in equation 16 and linear model is used for liquid phase (Eq. 17),

$$p = \rho RT \tag{16}$$

$$\rho = \rho_0 + \psi p \tag{17}$$

where ψ denotes compressibility of liquid phase.

Fully turbulent mixture in this study required a turbulent model to achieve comprehensive modeling and simulation. Large Eddy Simulation (LES) approach using one equation for finding Subgrid Scale (SGS) kinetic energy is employed as a turbulent model. This turbulent model is based on spatial filtering. The effect of small scale eddies, which are responsible for dissipation of kinetic energy are modeled and larger scale eddies which contains most of kinetic energy are directly solved. Smooth filtering coefficient of Δ is considered to be one with maximum Δ ratio of 1.1. Eddy viscosity and SGS kinematic viscosity are employed to approximate the SGS stress tensor where they both have a transport equation proposed by Yoshizawa and Horiuti [55] and described in equations 18 through 20:

$$\tau_{SGS} = \overline{UU} - \overline{U}\,\overline{U} \tag{18}$$

$$\tau_{SGS} = \frac{2}{3}k_{SGS}l = -\frac{\mu_{SGS}}{\rho}\left[\nabla\overline{U} + (\nabla\overline{U})^T\right] \tag{19}$$

$$\frac{\partial k_{SGS}}{\partial t} + \nabla.(k_{SGS}\overline{U}) = \nabla.[(\vartheta + \vartheta_{SGS})\nabla k_{SGS}] - \varepsilon - \vartheta_{SGS}S^2 \tag{20}$$

where ε, ϑ_{SGS} and S are calculated through following equations:

$$\varepsilon = \Delta C_\varepsilon (k_{SGS})^{3/2} \tag{21}$$

$$\vartheta_{SGS} = \Delta C_k (k_{SGS})^{1/2} \tag{22}$$

$$\bar{S} = \frac{1}{2}[\nabla\overline{U} + (\nabla\overline{U})^T] \tag{23}$$

where $C_\varepsilon = 1.05$ and $C_k = 0.07$.

2.2 Numerical setup and discretization

As it mentioned in previous sections, all the simulations results are obtained by using OpenFOAM code that uses cell center finite volume method. The procedure of solution is briefly based on the following algorithm:

```
┌──────────────────────────────────────────────────────┐
│        Creating the mesh field and variables field    │
└──────────────────────────────────────────────────────┘
                          │
                          ▼
┌──────────────────────────────────────────────────────┐
│  Adjusting of time step base on maximum courant       │
│  number defined by user                               │
└──────────────────────────────────────────────────────┘
                          ▼
            ┌──────────────────────────────┐
            │  Sovling Volume Fraction      │
            │  equation                     │
            └──────────────────────────────┘
                          │
          No      ◇ Converged ◇
                          │ Yes
            ┌──────────────────────────────┐
            │ calculating surface tension   │
            │ force and surface curvature   │
            │ after smoothing the surface   │
            └──────────────────────────────┘
                          ▼
            ┌──────────────────────────────┐
            │ Pressure Implicit with        │
            │ Splitting of Operators (PISO) │
            │ loop to calculate velocity    │
            │ and pressure                  │
            └──────────────────────────────┘
                          │
          No      ◇ Converged ◇
                          │ Yes
            ┌──────────────────────────────┐
            │     Calculating velocity      │
            └──────────────────────────────┘
                          ▼
            ┌──────────────────────────────┐
            │ Solving energy equation and   │
            │ obtaining compressibility of  │
            │ phases base on equation of    │
            │ state                         │
            └──────────────────────────────┘
                          ▼
            ┌──────────────────────────────┐
            │ Correct pressure and density  │
            │ base on compressibility       │
            └──────────────────────────────┘
```

As illustrated in the above figure, in the first step and after mesh construction, the time step for each iteration is adjusted according to the Courant number chosen by the user to guarantee the stability of solution as well as sufficient time marching step size. The time step is calculated by the following expression,

$$\Delta t = \min\left\{\min\left[\min\left\{\frac{Co_{max}}{Co_0}\Delta t_0, \left(1+\lambda_1\frac{Co_{max}}{Co_0}\right)\Delta t_0\right\}, \lambda_2\Delta t_0\right], \Delta t_{max}\right\}$$ (24)

where the Courant number is computed by,

$$Co = \frac{|U_f.S_f|}{d.S_f}\Delta t$$ (25)

S_f and d refer to the normal surface area vector, and the vector between calculation points of the control volumes with faces in common, respectively. Two damping factors, λ_1 and λ_2 , are defined to limit the high time step oscillations, which results in the instability of solution. It should be noted that initial time step size of 10^{-7} (s) is chosen for these simulations to ensure the stability of solution

In this simulation, time derivative terms are discretized by utilizing the second order implicit backward scheme. A second order central differencing scheme, Gauss limited linear scheme, is used for divergence terms which uses Gauss' theorem. The pressure gradient is discretized with least square scheme.

2.3 Initial and boundary conditions

At the starting point to simulate the experimental condition, as if we start the simulation from injection of liquid into the nozzle, it is not computationally effective on

33

final result, the distribution of volume fraction is defined at the initial time. The definition of interface and volume fraction is made in a way that the nozzle is entirely full of water. All the initial velocity and pressure is set to be zero and at atmospheric pressure, respectively. As it is depicted in Fig. 2-2, the liquid phase is injected into the nozzle through the upper inlet with the constant mass flow rate. The air phase is introduced to the mixing chamber with constant mass flow rate as well from smaller surface at the end of the tube in the middle of nozzle. The nozzle walls are set to have no slip condition for velocity and zero gradient for pressure. The top blue surface is set to be as a wall according to experiment and other side and bottom surfaces are set to be as total pressure and pressure velocity outlet for pressure and velocity (far field), respectively.

Liquid Air Liquid

Top wall

Discharge

Far field

Far field
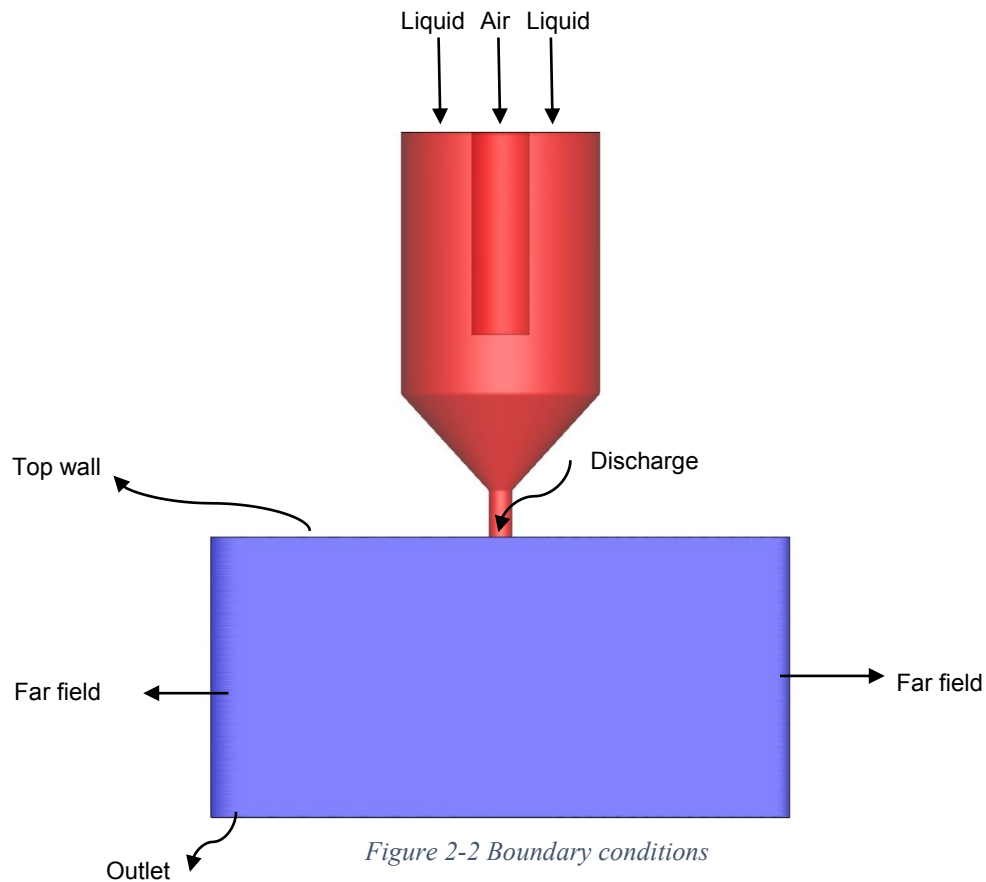
Figure 2-2 Boundary conditions

Outlet

All the simulations have been carried out in 3-D unstructured hexahedral and polyhedral mesh using local refinement in order to avoid unnecessary computations. The mesh is shown in Fig. 2-3 and 2-4. The mesh size in the refined part is in the range of 20 to 30 μm. It should be noted that all the simulations are performed using Compute Canada [56] resources. Due to the limitation of resources, capacity of our infrastructures and also in order to avoid higher computational cost and longer computational time, it was the maximum refinement level that the simulation could be performed. The mesh is generated by ICEM-CFD, which is part of ANSYS software package.
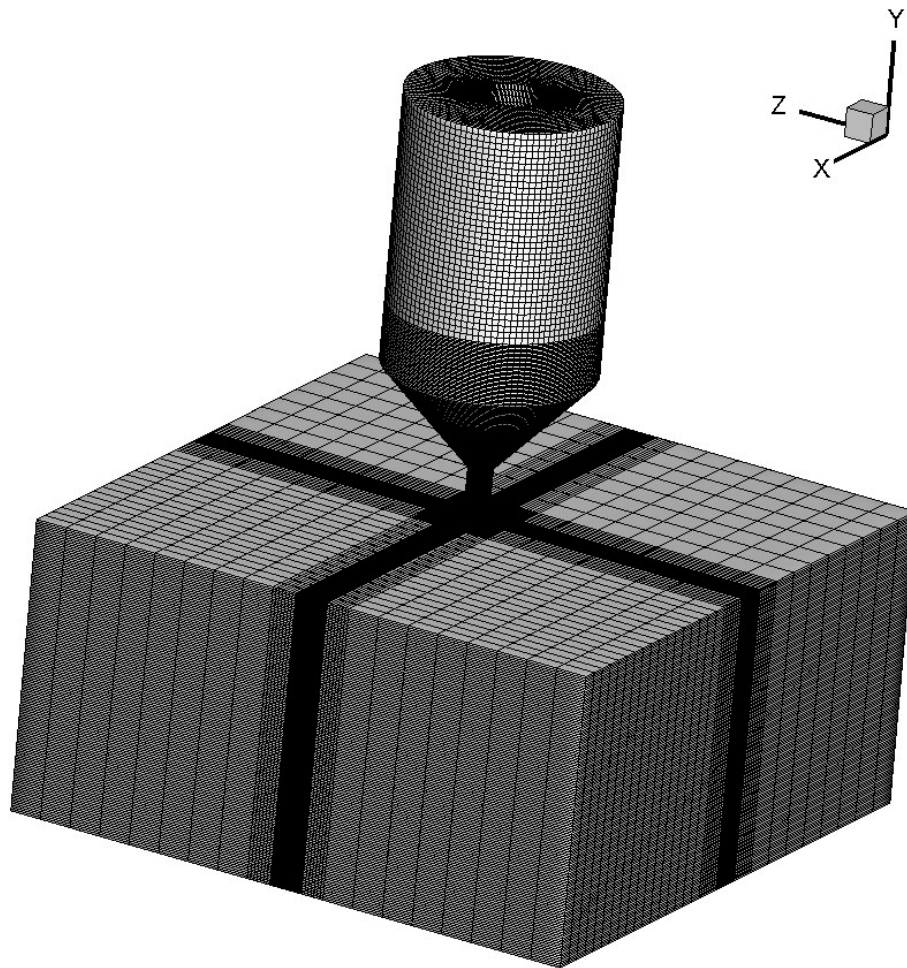

*Figure 2-3 Computational inside and outside the Effervescent nozzle*
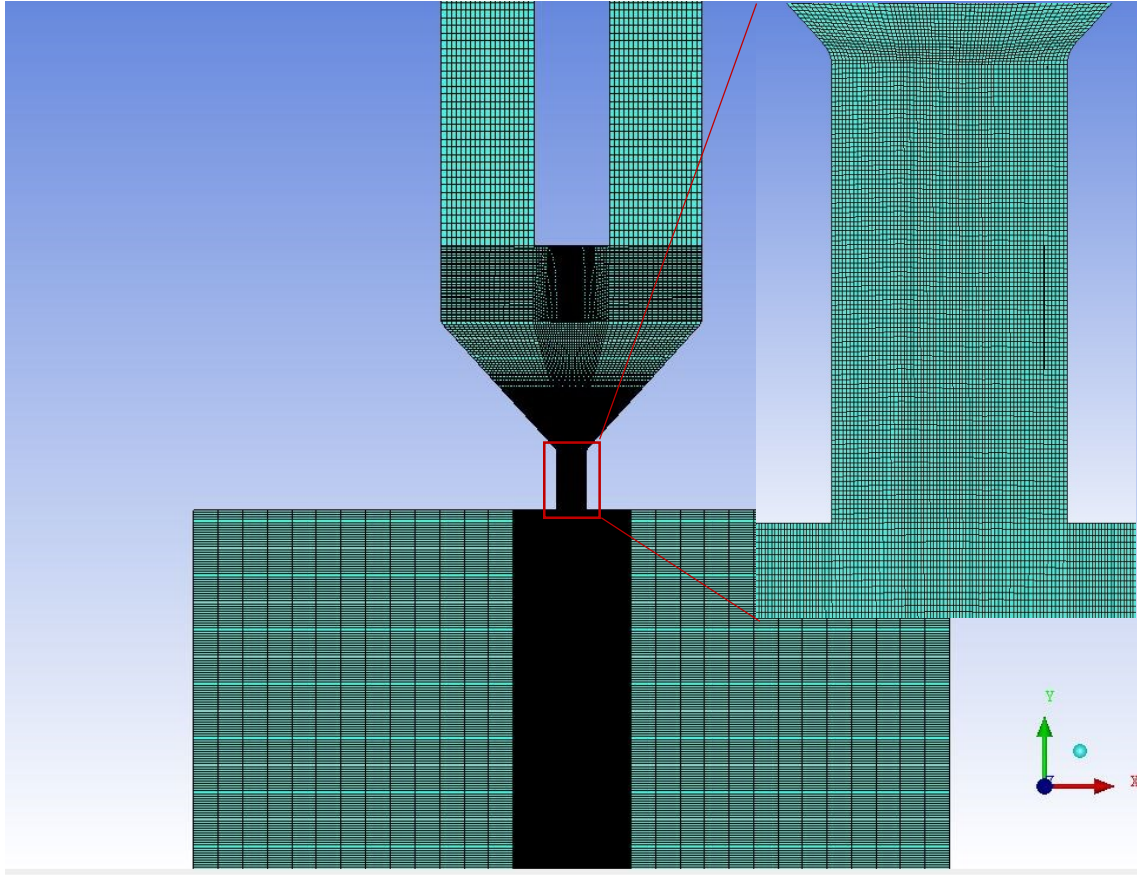
Figure 2-4 Mesh slice showing local refinement

In this study, water and air are used as the liquid and aerating gas, respectively. Liquid is injected at a constant mass flow rate of 0.0133 kg/s (i.e. 800 mL/min) and air is injected according to GLR. Based on GLR, the mass flow rate of gas phase adjusted, which is tabulated in table 2-1. The k values of turbulence flow for inlets are obtained using equation 26 where "I" refers to the turbulence intensity. The value of turbulence intensity for liquid inlet assumed to be at low level of 2% as the velocity and Reynolds number are low. This value for air inlet is considered to be relatively higher (i.e. 10%) due to high velocity of air phase.

$$k = \frac{3}{2}(UI)^2 \qquad (26)$$

Table 2-1 Mass flow rate of injected gas

GLR (%)	Gas mass flow rate $(\frac{kg}{s})$
0.55	2.56e-5
1.1	13.95e-5
1.6	16.8e-5
2.6	27.72e-5

Once the simulation is performed for pure water as an operating fluid, the next step is to study the effect of fluid properties by resembling suspension properties such as density, viscosity and surface tension. The results of experimental measurements carried out previously in Tabrizi's MASc. thesis [57], in Concordia University Multiphase Flow Lab are used. It should be mentioned that the suspension is prepared by suspending 20-80 micron size glass beads in solution of Water/Glycerol. The corresponding data of the measurement used in this study is shown in Table 2-2. For further information about the preparation and measurements, refer to Tabrizi's Thesis [57].

Table 2-2 Rheological properties of suspension [57]

Liquid properties (At 20 ℃)		**Suspension**
Density	$\rho\ (kg/m^3)$	1273.2
Dynamic viscosity	$\mu\ (N.s/m^2)$	9.17×10^{-3}
Kinematic viscosity	$\vartheta\ (m^2/s)$	7.25×10^{-6}
Surface tension	$\sigma\ (N/m)$	5.7×10^{-2}

3 Results and Discussion

In this chapter, the results of Effervescent atomizer for internal and external flow are discussed. The effects of GLR on the Internal flow structure, liquid film thickness, primary atomization, breakup length, cone angle and the average velocity of flow are investigated.

At the outset, the structure of the internal flow is investigated in order to achieve fundamental understanding of the phenomena happening in Effervescent sprays. Study of internal flow includes the flow pattern in the discharge orifice, liquid film thickness and finally the pressure variation inside the nozzle during atomization. For the last section, unsteadiness and critical conditions for the choked flow inside the Effervescent nozzle are investigated. Afterwards, the corresponding spray characteristics of the Effervescent atomizer such as: spray cone angle, breakup length, primary atomization, velocity profile, penetration and spray pattern are investigated. Finally, the effect of liquid properties is partially studied to obtain a comprehensive understanding of the phenomena occurring in Effervescent sprays.

3.1   Internal flow

At the beginning of the simulation of different cases, the water and air are injected to the nozzle filled by water, from different inlets. As time goes on, the external jet of water is forming along with the bubble formation inside the nozzle. Depending on the airflow rate, the time when the air reaches to the end of converging part differs. Whenever the air reaches the orifice passage, various patterns of two-phase flow are formed in the discharge passage depending on amount of GLR.

3.1.1 Flow pattern in the orifice

Characteristics of external flow in effervescent atomization such as breakup length, primary-secondary atomization, cone angle and velocity are governed by the flow structure inside the nozzle. Different parameters such as the nozzle geometry (i.e. mixing

chamber size, aerator holes size, numbers and location), GLR and fluid properties have significant influence on the type of internal flow. The initial regime in the nozzle is bubbly flow, where the small bubbles grow upon passing the discharge orifice and their consequent sudden burst results in liquid fragmentation i.e. atomization. As illustrated in Fig.s 3-1 and 3-2, the effect of GLR on internal flow pattern is compared to Tabrizi's experiments [57].
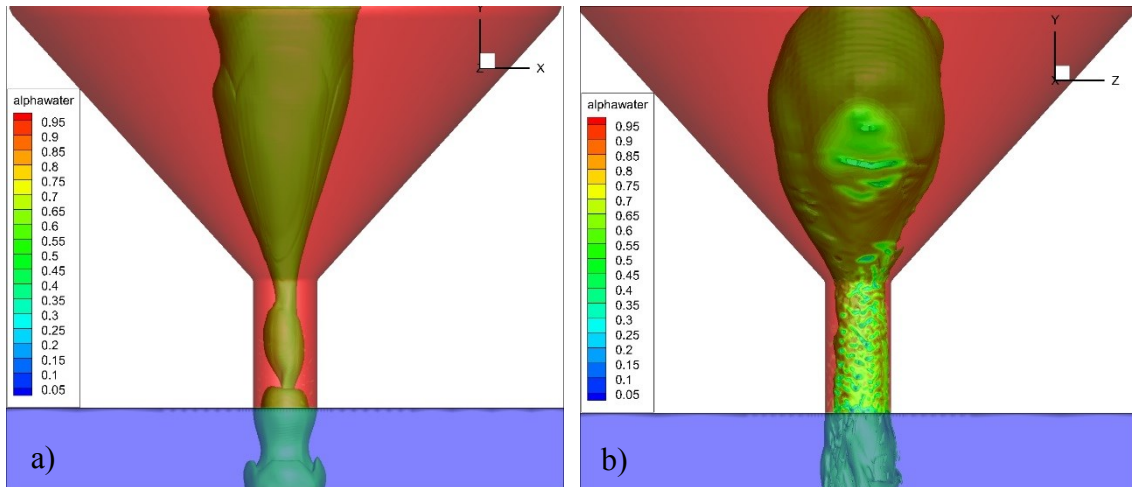

Figure 3-1 Pattern of the internal flow a) bubbly flow and b) annular flow
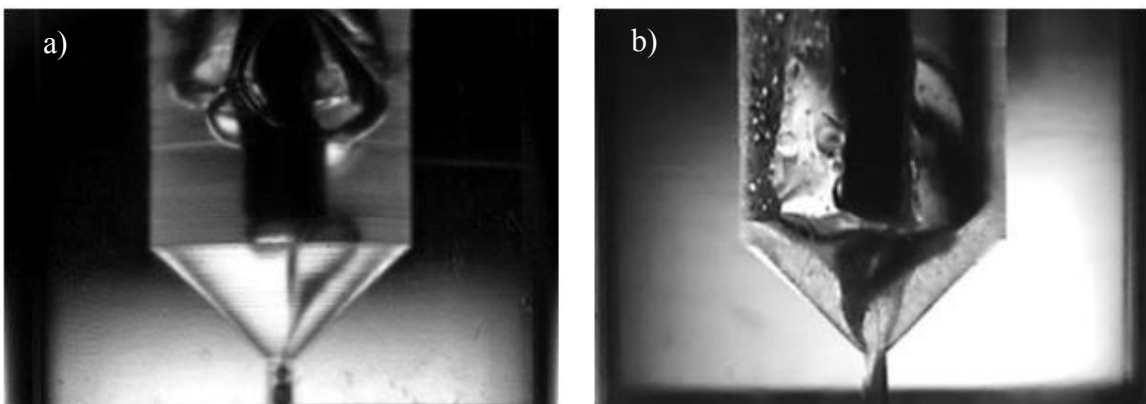
Figure 3-2 The experimental results of the internal flow a) bubbly flow b) annular flow courtesy of Tabrizi

[57]

In figure 3-1, the iso-surface of volume fraction of 0.5 represents the interface between two phases. It should be noted that Tabrizi [57] employed high-speed camera and shadowgraphy technique to capture and post process the images in figure 3-2.

The comparison shows that at low GLRs (i.e. 0.55%), the bubbles are stretching in the mixing chamber due to high pressure and low velocity and then form bubbles in the orifice discharge which leads to bubble bursting outside the nozzle. This regime is categorized as the bubbly flow (Fig. 3-1-a). By further increase in GLR (i.e. 1.1%, 2.6%), the flow is altering to the annular flow where a core of gas flow is surrounded by a thin layer of liquid sheet (Fig. 3-1-b). The results are in a good agreement with Tabrizi's [57], and Roesler and Lefebvre's experiments [18].

Due to complexity and computation time required for capturing pure bubbly flow, in our simulation, the effect of bubbly flow (close to transient flow) at the discharge orifice and outside is captured. The bubble detachment in the passage of the discharge orifice and bubble stretching are shown in Fig. 3-3. At the beginning, bubble starts growing in the mixing chamber and then stretching towards the orifice passage (Fig. 3-3-a). As the velocity increases at the beginning of the discharge orifice, the detachment of bubble initiates (Fig 3-3-b). Due to lower pressure in the discharge passage, the detached bubble expands gradually which result in pressure variations (Fig 3-3-c). Finally, the bubble suddenly expands upon exiting the discharge orifice, which results in bubble bursting downstream the nozzle (Fig 3-3-d).
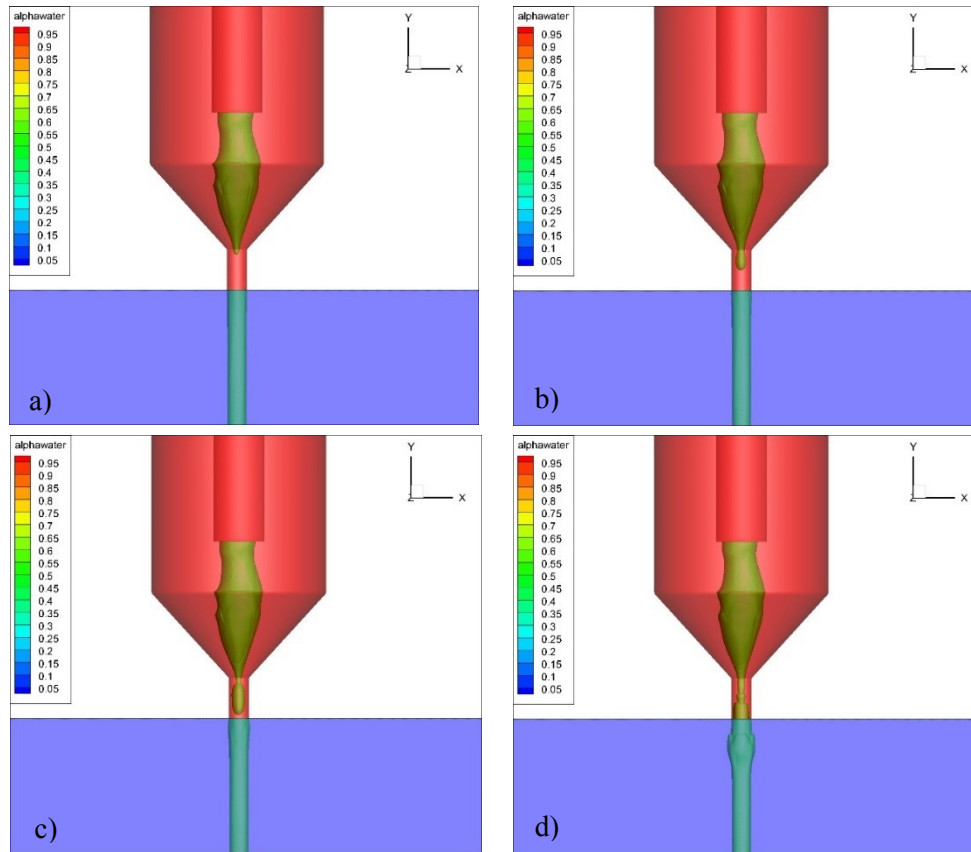
Figure 3-3 Sequences of bubble formations to bubble bursting for GLR=0.55%, a) bubble stretching, b)

bubble formation, c) bubble detachment, and d) bubble expansion

3.1.2 Liquid film thickness

One of the immense parameters of internal flow affecting the quality of primary atomization and final droplets is the thickness of liquid film upon exiting the discharge orifice. In addition, one of the effective parameters on liquid thickness is the level of GLR. The effect of variation of GLR on the liquid film thickness is more significant in relatively lower GLRs. After reaching to certain level, any further increase in GLR leads to the slight reduction in the thickness. In this section, the thickness of liquid film in the discharged passage is numerically studied. Lin et al. [58] has experimentally investigated the effect of various GLR levels and the liquid flow rate on liquid film thickness in a

square cross-section Effervescent atomizer. They proposed an empirical equation base on the gas flow rate. It should be noted that their formulation is only valid in their experimental range.

For calculating the liquid film thickness, the difference between diameter of the gas core and surrounding liquid sheet is averaged through time and the final value is compared to the experimental results of Lin et al. [58].

$$t = \frac{1}{2}\left(D_O - D_g\right) \tag{27}$$

where t is liquid thickness, D_O is the diameter of discharge orifice and D_g is the diameter of gas core. It should be noted that the value of D_g is calculated by averaging the area, where gas core has occupied at the discharge orifice and calculating the equivalent diameter. For example, the liquid film thickness for GLR=2.6% at the exit plane of the discharge orifice is shown in Fig. 3-4, where the α is volume fraction with the range of unity for liquid phase and zero for gas phase. For higher GLRs, the measurement of gas core diameter is easier since there are fewer oscillations in the diameter by time. The determined liquid film thickness compared with the proposed correlation base on gas flow rate by Lin et al. [58] is described in Fig. 3-5. As shown, the measured simulation data are in good agreement with the empirical correlation and have the same trend as the experimental results.
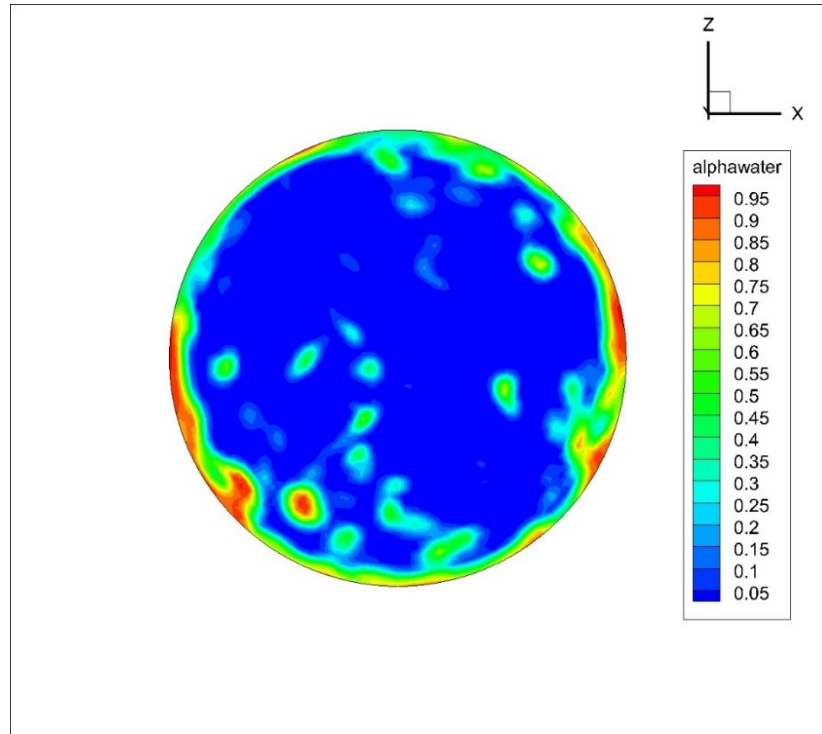
*Figure 3-4 Liquid film thickness for GLR=2.5%*
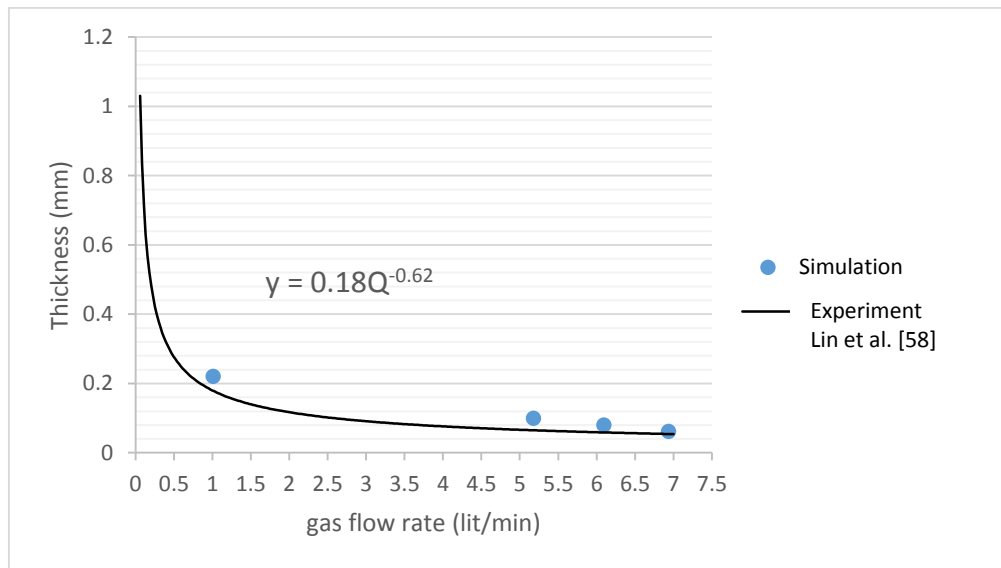
Figure 3-5 Comparison of numerical results with the experimental results of Lin et al. [58]

It should be noted that Lin et al. [58] used a square cross-section nozzle for better shadowgraphy purposes. However, for calculation of film thickness, they considered the

hydraulic diameter to relate it to more practical cylindrical discharge orifice. Both results demonstrate the immense effect of aerating gas flow rate on liquid film thickness. As it is shown in Fig. 3-5, variations in lower range of GLRs lead to rapid variations in film thickness, whereas the further increase in higher range of GLRs results in slight change in liquid film thickness. The advantage of thinner liquid film is quicker break up of liquid sheet and consequently smaller droplets with higher velocity. Having small droplets is beneficial in different applications such as drying, combustion and particularly, our interest, suspension thermal spray. In suspension thermal spray where the suspension is a method to inject nano-size particles through liquid into a plasma plume, having smaller droplets is beneficial as they contain smaller amount of particles. The smaller amount of particles leads to the smaller size particle agglomerations after rapid evaporation of liquid phase. The smaller the droplets, the smaller produced agglomerated particles, which results in better particle distributions and higher quality coatings.

3.1.3 Internal thermo physical properties

One of the challenging issues of understanding the principal of effervescent sprays is to understand the internal flow thermo-physical properties such as pressure gradients, velocity change, temperature, and critical condition of flow inside and outside of the nozzle. Prediction of flow condition based on the liquid volume fraction has a significant influence on the external flow characteristics. In this section, the pressure change inside the nozzle along with temperature and critical conditions are studied. Chawla [27] has reported that however the speed of sound in single-phase flow for water and air is respectively 1300 m/s and 300 m/s, the speed of sound has a sudden decrease in two-phase flow mixture where the it reaches the value as low as 20 to 30 m/s. The

consequence of this critical condition is the pressure jump occurring at the orifice exit. This relatively higher-pressure difference at discharge orifice exit results in a sudden expansion of the gas phase and breakup of the liquid even in lower velocities. In order to predict the critical pressure, the equation proposed by Churchill and Usagi [59] is used to obtain critical pressure ratio,

$$\frac{P_c}{P_0} = \left[\left(\frac{\kappa + 1}{2} \right)^{\frac{4\kappa}{3(\kappa-1)}} + \left(\frac{\kappa}{2} \frac{1 - \alpha_0}{\alpha_0} \right)^{\frac{4\kappa}{3(\kappa+1)}} \right]^{-\frac{3}{4}} \tag{28}$$

where κ is the specific heat ratio of gas and α_0 denotes gas volume fraction which can be calculated by gas flow rate and to total flow rate ratio.

$$\alpha_0 = \frac{Q_g}{Q_l + Q_g} \tag{29}$$

The volume fraction and critical pressure are calculated for various GLRs. The numerical results show that the Effervescent nozzle is too unsteady and frequently works in the critical condition. At the beginning of the process, the pressure of the nozzle increases to the maximum pressure depending on the GLR value (i.e. gas injection pressure). The internal pressure of the nozzle gradually decreases upon exiting of the air phase. Few samples of the pressure variation are shown in Fig. 3-6.
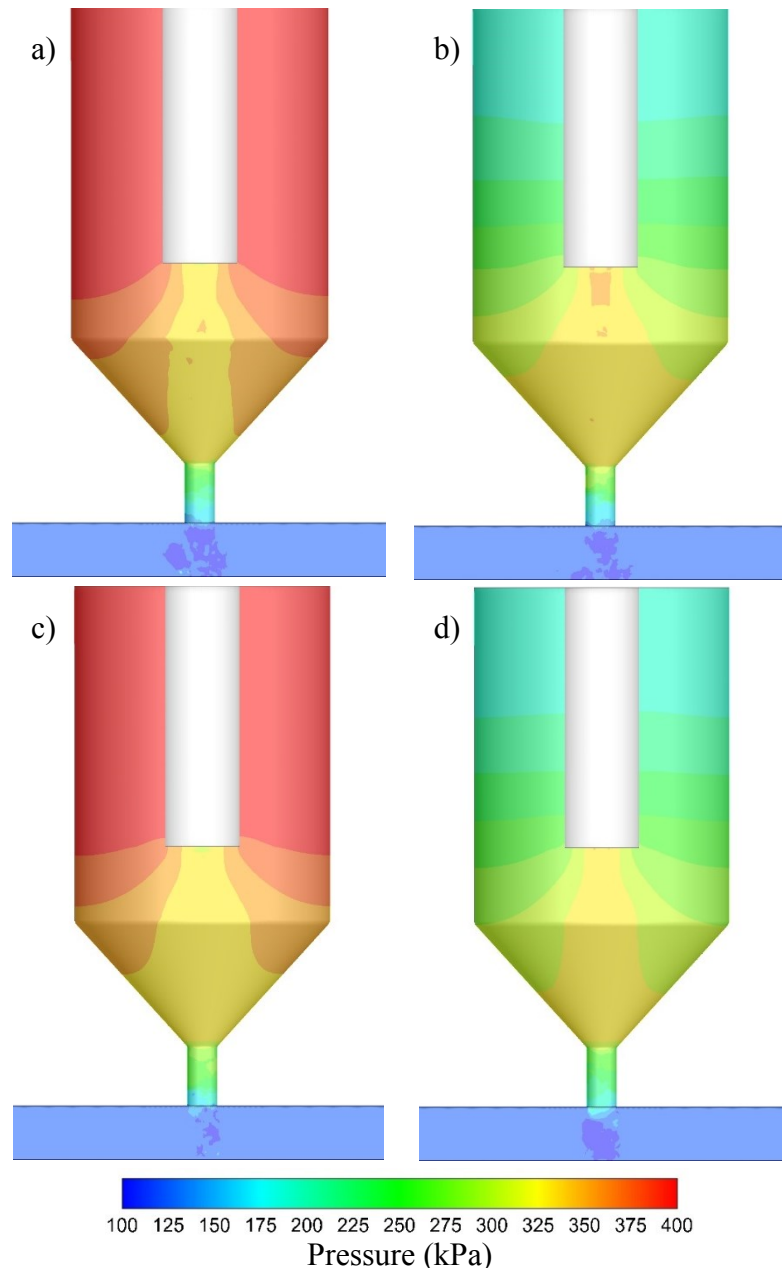
Figure 3-6 Pressure variations inside the nozzle upon exiting of air phase from the discharge passage for

GLR=2.6% at time= a) 2.2 b) 2.25 c) 2.3 d) 2.35 ms

Within the few starting steps, when the gas reaches the discharge orifice, the pressure in

the nozzle is at the maximum point. Nevertheless, through further additional time steps,

the internal pressure of the nozzle decreases to reach to a stable pressure. It is obvious

that by reaching the critical condition inside the discharge orifice, few oscillations inside

the nozzle occur. This creates the unsteadiness behavior of the Effervescent nozzle. In Fig. 3-7 and 3-8, the variations of pressure and temperature in later time steps are depicted for a GLR = 2.6%.
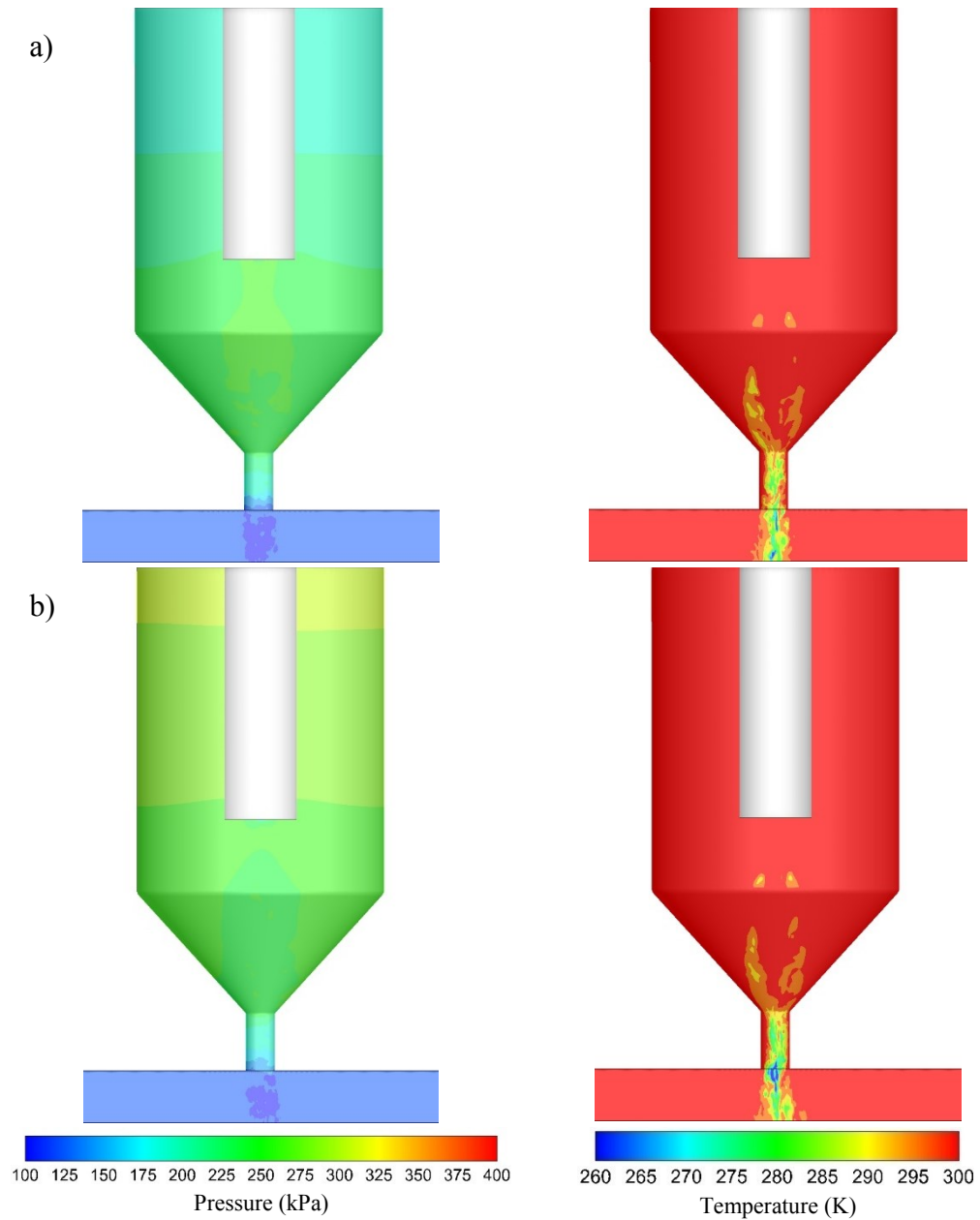
Figure 3-7 Pressure and corresponding temperature variations in later time steps for GLR=2.6% a)

time=3.25 b) time=3.3 ms
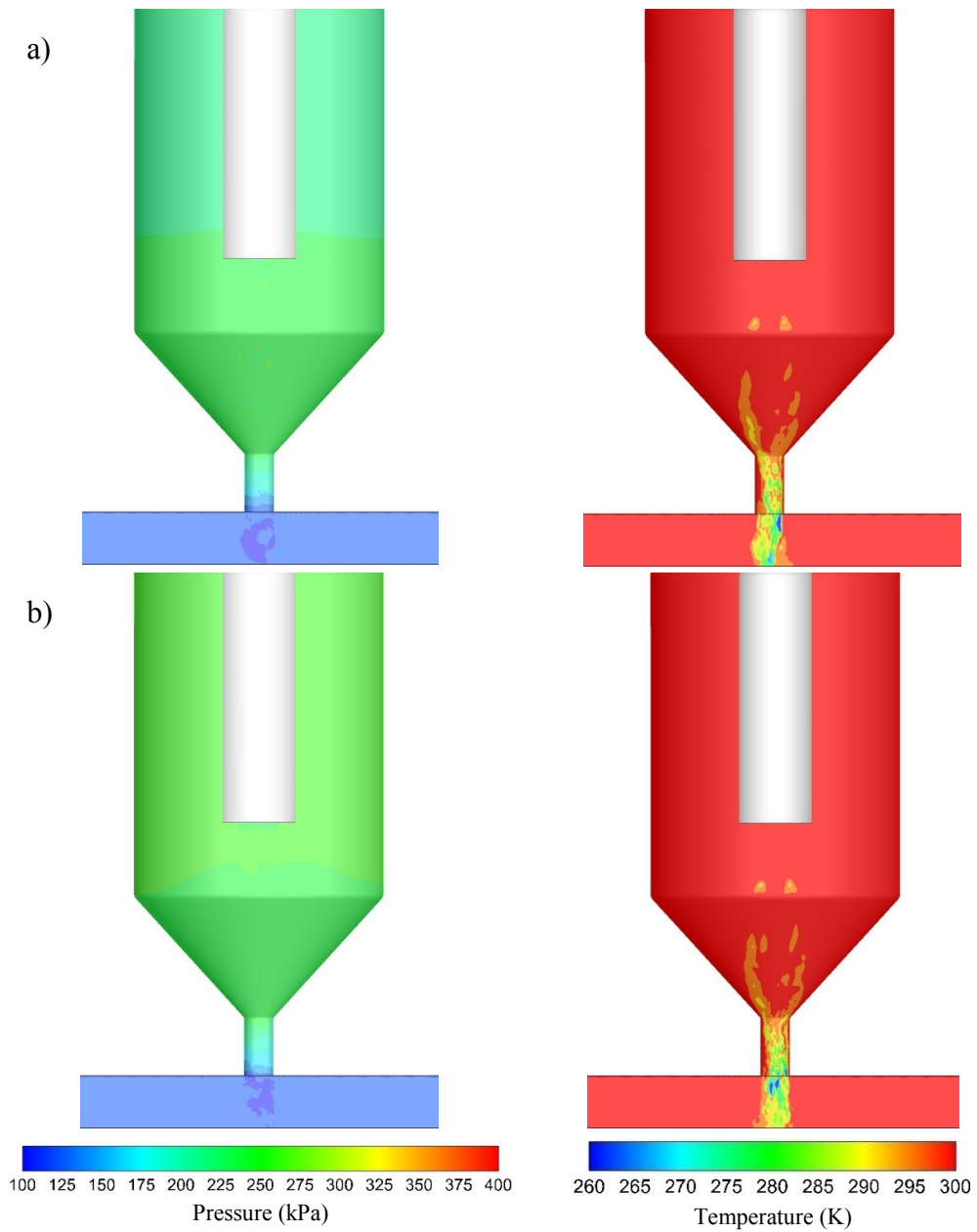
Figure 3-8 Pressure and corresponding temperature variations in later time steps for GLR=2.6% a)

time=3.35 b) time=3.4 ms

As it is illustrated in the above two figures (Fig. 3-7 and 3-8), the pressure variations

inside the nozzle is accompanied with the temperature variations, particularly in orifice

passage where the pressure changes are significant. The same happens at the discharge orifice where a pressure jump occurs due to the choked flow. Because of high expansion rate and high velocity of the gas phase at the discharge orifice, the temperature drops suddenly. In addition, both temperature and pressure show an oscillatory behavior inside the orifice exit. The oscillatory behavior of the internal pressure at the different positions of the nozzle is captured by extracting data through time. The positions of investigation points are shown in Fig. 3-9.
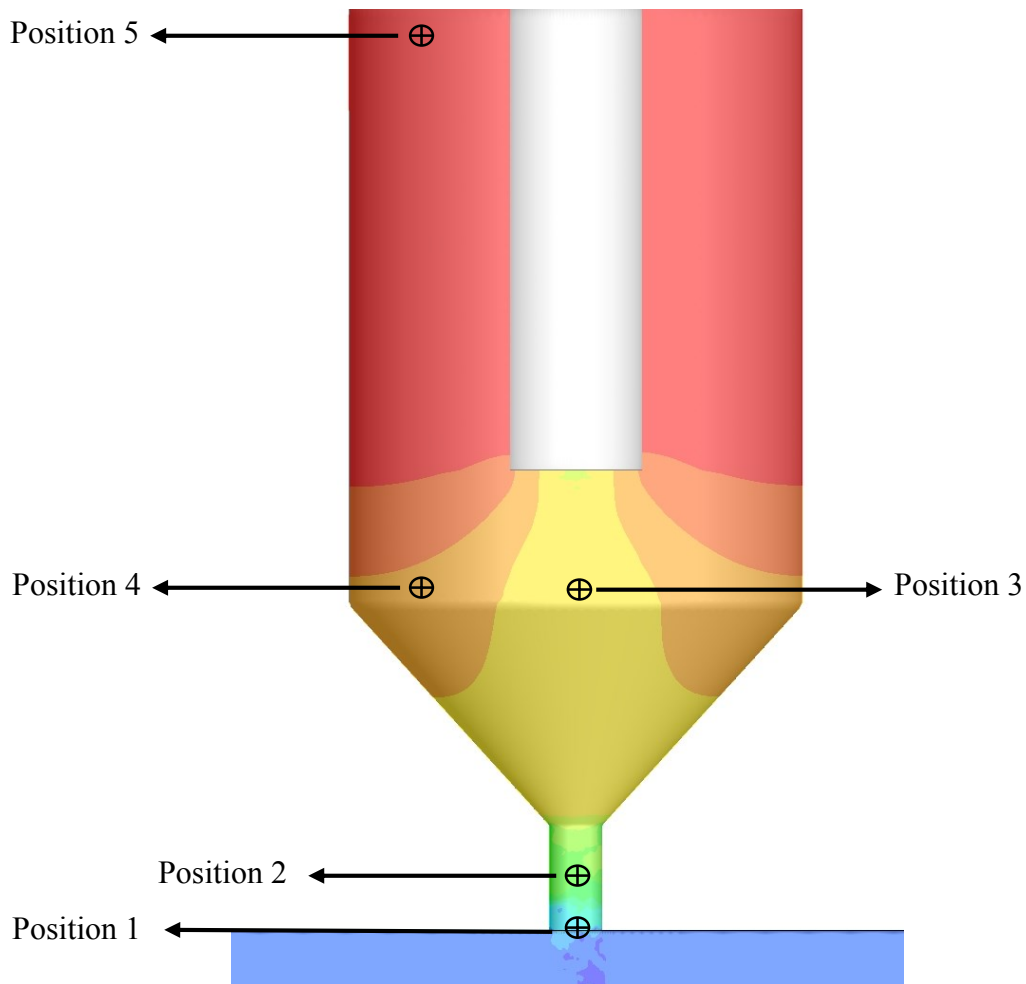

Figure 3-9 Positions of investigation points

In Figs. 3-10 and 3-11, the oscillatory behavior resulting from the effect of choked flow at discharged orifice is shown.
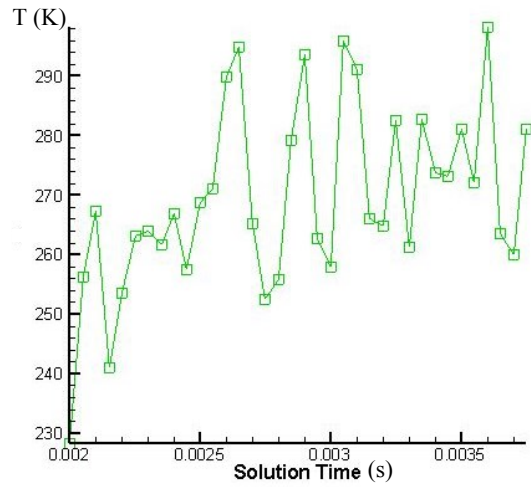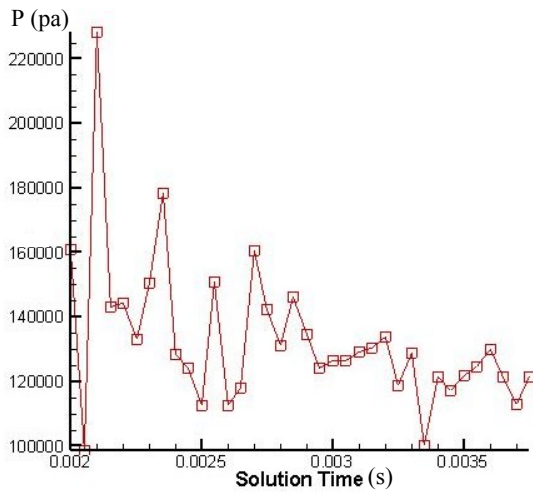
Figure 3-10 Pressure and temperature variations at the discharge orifice (position 1) for GLR=2.6%
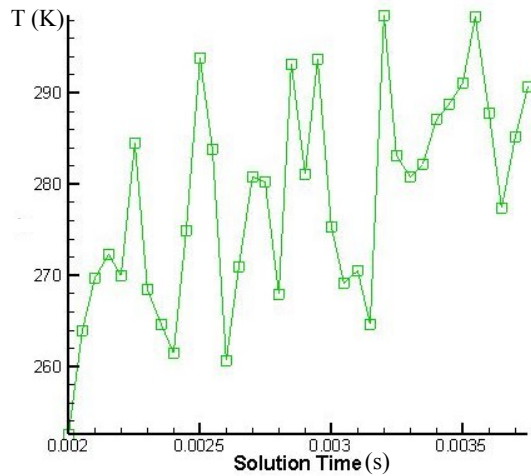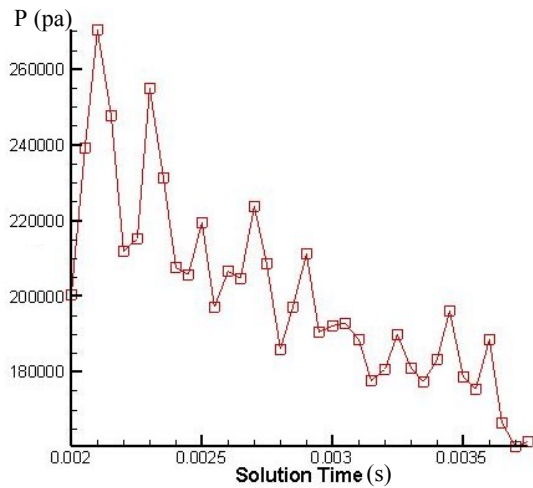

Figure 3-11 Pressure and temperature variations in the middle of the orifice discharge passage (position 2)

for GLR=2.6%

The two Figures, 3-10 and 3-11, show the instabilities of the pressure and consequently temperature at the discharge orifice as well as pressure differences between the discharge orifice and ambient. Those are due to choked flow occurring at the nozzle exit. The mixture reaches a sonic condition even in much lower velocities [27], the flow in Effervescent nozzle reaching to its critical condition that almost obeys the critical

51

pressure ratio proposed by Churchill and Usagi [59]. Those oscillations transmit to liquid and gas interface that result in waves on the interface and consequently breakup of the liquid sheets upon exiting from the discharge orifice. At a certain point, such as the time between 2.9 to 3.2 ms, the flow inside the Effervescent nozzle shows a partial stability and steadiness. However, this behavior does not last for long, and the instabilities further grow and finally the flow reaches again to its critical condition. According to the comparison of pressure variations at the discharge orifice and the mixing chamber, which determines the average pressure for calculating critical pressure, Fig. 3-12, the small variations of discharge pressure lead to small variations in the gas phase; however these variations boost for the liquid phase.
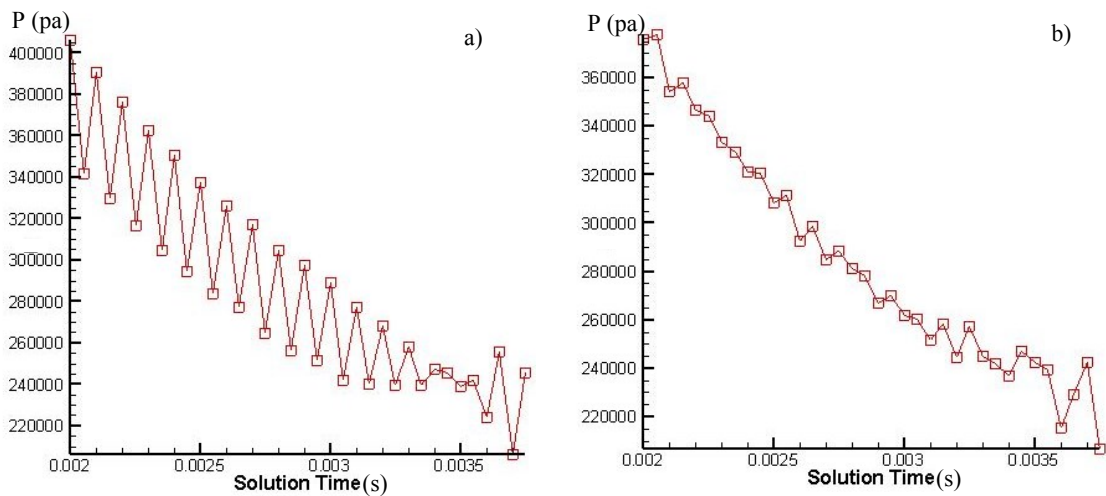

Figure 3-12 Pressure variations in the mixing chamber a) in the liquid phase (position 4) b) in the gas phase (position 3) for GLR=2.6%
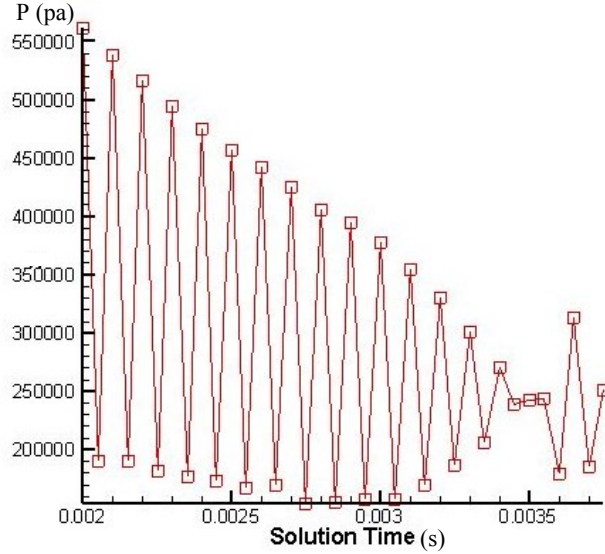
Figure 3-13 Pressure variations near the liquid inlet (position 5) for GLR=2.6%

The boosted pressure variations for the liquid phase in the mixing chamber result in oscillatory pressure alternations at the liquid inlet to maintain a constant mass flow rate. However, maintaining this constant mass flow rate in the practical situation is not possible. This causes more instability in Effervescent nozzle. Although the large variations occurred in liquid inlet, the average pressure is around three time the atmosphere pressure, which is equal to the measured pressure by Tabrizi [57]. The frequent variations of the inlet pressure in the simulation probably can be used for calculating the frequency of the choked flow occurring at the nozzle exit, though, it requires further studies to relate this frequency to the working condition frequency of the Effervescent nozzle. In addition, the effect of different GLRs can be deduced in the following figures where two other GLRs of 1.1% and 0.55% are studied.
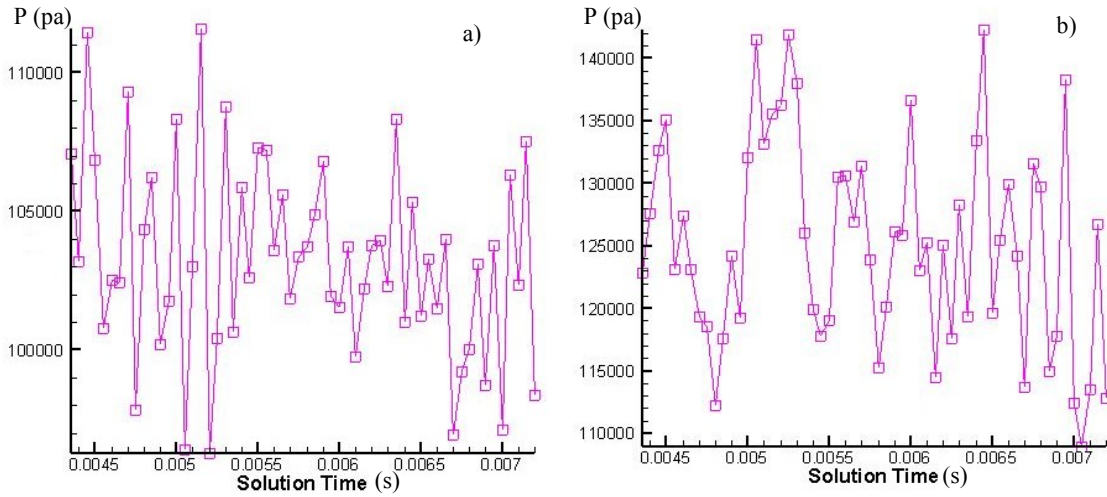
Figure 3-14 Pressure variations at a) the discharge orifice (position 1)

b) the middle of the discharge passage (position 2) for GLR=1.1%
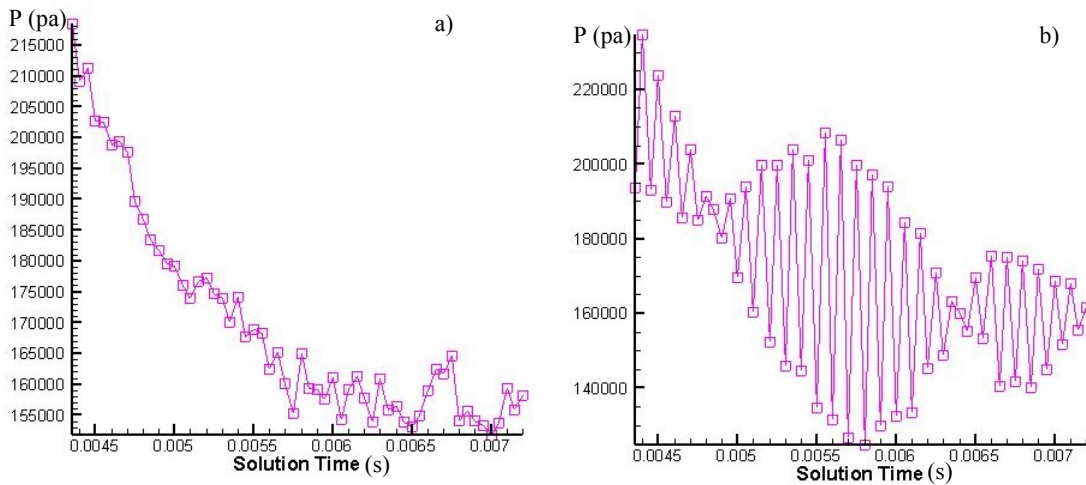

Figure 3-15 Pressure variations in a) the mixing chamber (position 3)

b) near the liquid inlet (position 5) for GLR=1.1%

For a GLR value of 1.1%, the amplitude of the oscillations and the average pressure shows a decrease in comparison to higher GLRs. The effect of lower amplitude of oscillations at the nozzle exit results in lower amplitude of oscillations in the mixing chamber and consequently lower magnitude of oscillation at the liquid inlet to maintain a

54

constant mass flow rate. In addition, lower amplitude of oscillations results in lower rate of expansion of the gas phase upon exiting from the discharged orifice and consequently a smaller cone angle. By further reduction in the flow rate of injected gas, the mixing chamber and the overall nozzle pressure decreases and the frequency of instabilities decreases for higher GLRs, this effect is depicted in Fig. 3-16.
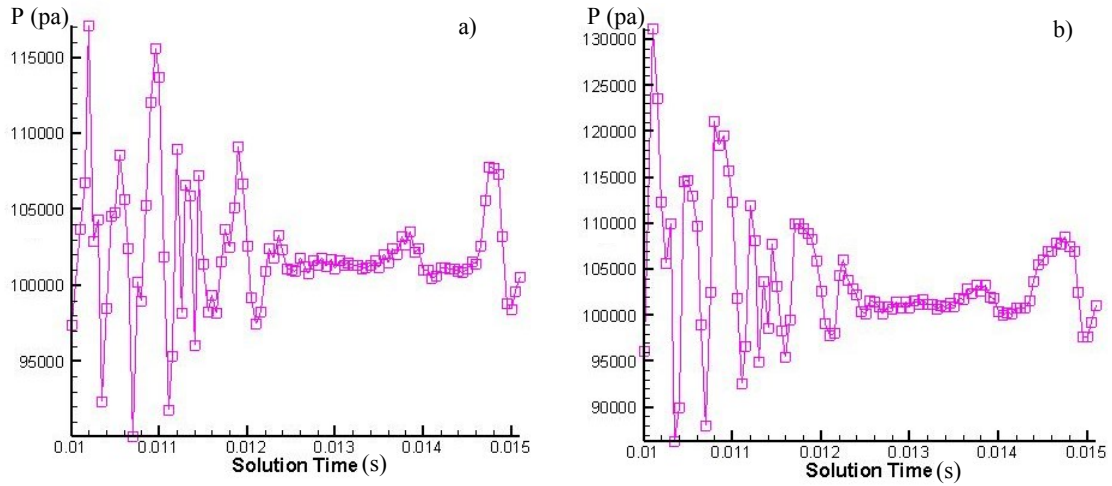

Figure 3-16 Pressure variations at a) the exit orifice (position 1) b) the middle of discharge passage

(position 2) for GLR=0.55%
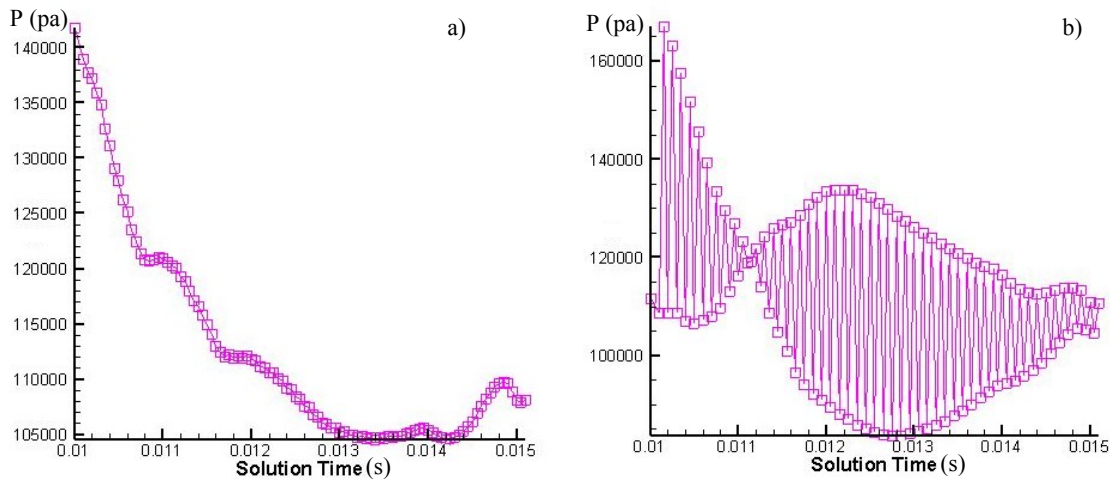
Figure 3-17 Pressure variations in a) the mixing chamber (position 3) b) the liquid inlet (position 5) for

GLR=0.55%

For GLRs less than 0.55% where the flow is nearly bubbly flow, the trend of decreasing the magnitude of oscillations by reducing the GLR is evident. The effect of lower GLR is more obvious in the mixing chamber pressure oscillations where these oscillations are almost omitted. However, once a large bubble leaves the orifice discharge, the pressure has few peaks, which are due to the flow choking. The trend of pressure variations demonstrates that the GLR effect is more on frequency and magnitude of the operating conditions of the Effervescent nozzle. This unsteadiness is beneficial in suspension injection where the steady injectors struggle with clogging problem while the unsteadiness and pressure changes in an Effervescent nozzle serves as a self-cleaning mechanism. The effect of liquid properties on the pressure variation is shown in Figs 3-18 through 3-20.
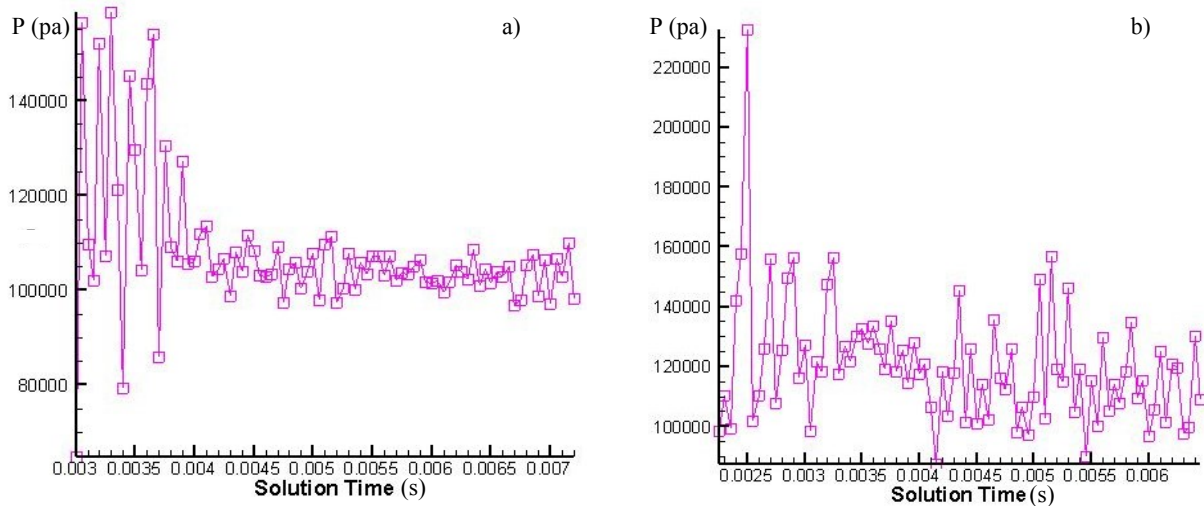

Figure 3-18 Pressure variations at the orifice exit (position 1) for GLR=1.6% a) water b) suspension
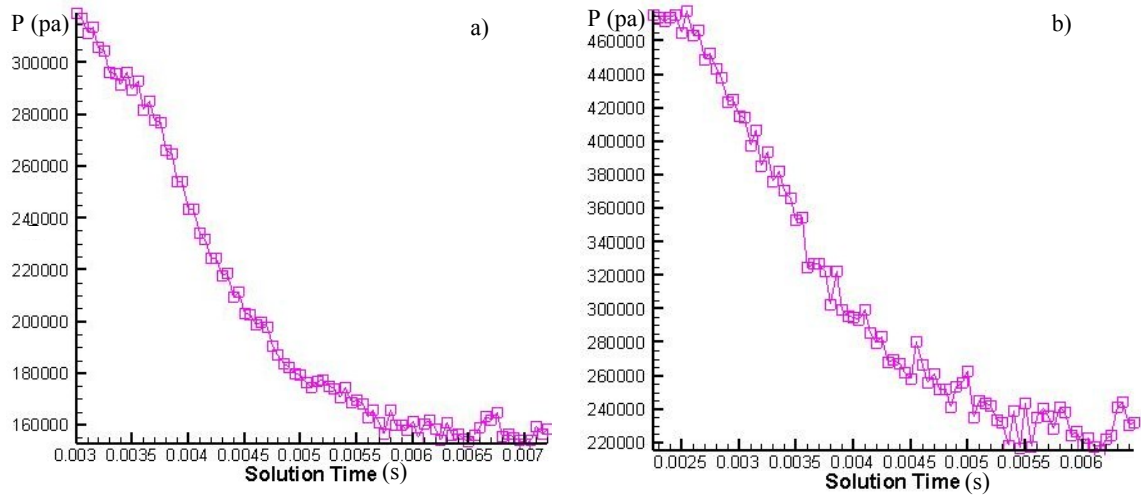
Figure 3-19 Pressure variations in the mixing chamber (position 3) for GLR=1.6% a) water b) suspension
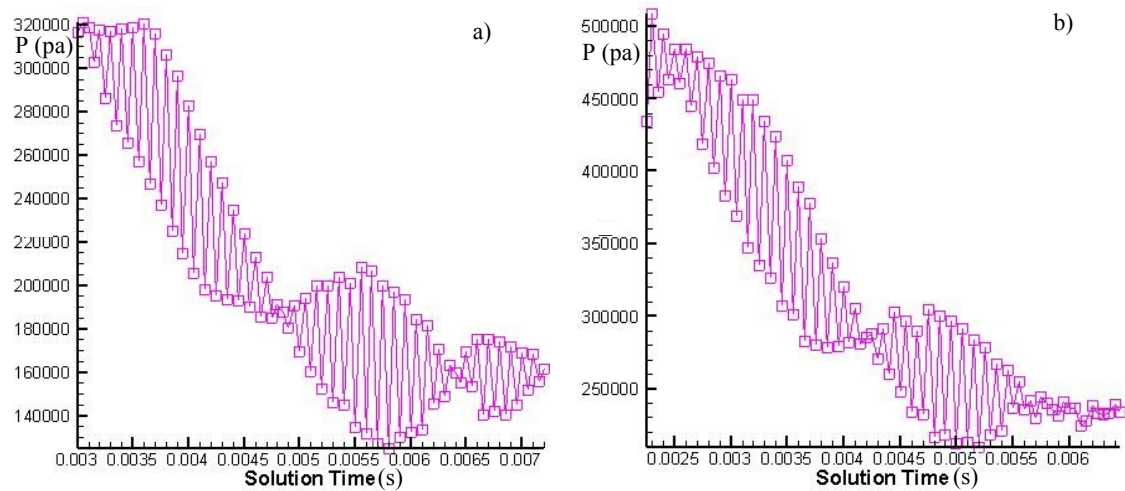
Figure 3-20 Pressure variations at the liquid inlet (position5) for GLR=1.6% a) water b) suspension

The three figures, (i.e. Fig. 3-18 to 3-20), are used to compare the characteristics of the spray formed by water and suspension. The average pressure, pressure oscillations and pressure jump occurring at the orifice exit are demonstrated. The instance effect of the higher viscosity and density associated with suspension spray is revealed in the average pressure, which is higher for the suspension case. On the other hand, the rate of dissipation of oscillations in the liquid phase of the suspension is more than that of water.

Furthermore, the oscillations in the gas phase in the mixing chamber for the water case is less than the suspension case, which is believed to be due the to lower surface tension of the suspension. Moreover, the suspension/air mixture at the discharged orifice faces three times higher magnitude of oscillation due to lower surface tension. The first consequence of higher-pressure jumps and more oscillations will be wider cone angle in the downstream of spray and more turbulence at the interface of liquid/gas. In next section, these effects on the cone angle and the velocity profile are studied.

3.2 External flow

The perspective of this section is to study numerically the effect of various GLRs and liquid properties on the primary atomization parameters i.e. breakup length and cone angle. Furthermore, the relationship between the internal flow and these parameters is comprehensively discussed. Finally, the velocity of liquid and air are investigated in the near field for variuos GLRs.

3.2.1 Liquid Breakup length and cone angle

At the outset, the first set of images, Fig. 3-21, demonstrates the variation of breakup length according to GLRs. For lower GLRs (i.e. GLR = 0.55%) the bubble gradually expands upon exiting from the discharge orifice due to the pressure jump. This gradual expansion results in longer breakup length whereas by further increase in GLR, the internal flow pattern changes. The transition from bubbly flow with random breakups to the annular flow by further increase in GLRs, lead to steadier and shorter breakup length.
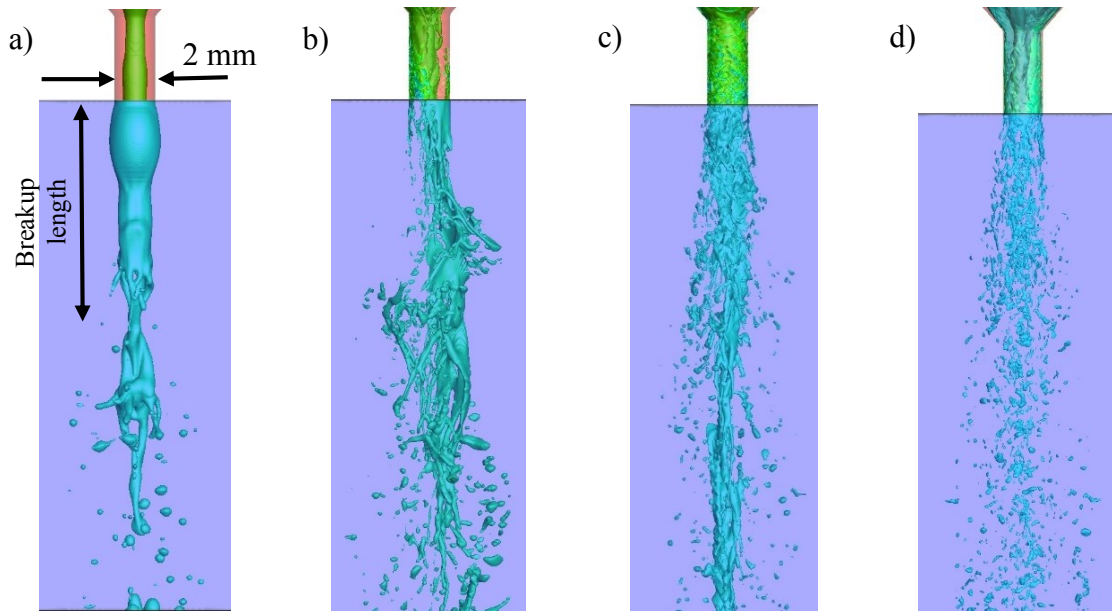
Figure 3-21 Breakup length for various GLRs of a) 0.55 b) 1.1 c) 1.6 and d) 2.6%

It should be noted that the mechanism of breakup from low GLR to higher GLR alters from breakups due to bubble expansion to breakup due to high interface disturbances in higher GLRs. These mechanisms of breakups are in agreement with the experimental results of Buckner and Sojka [25], Santangelo [38], and Tabrizi [57]. The breakup lengths are averaged through the time. Fig. 3-22 shows that the breakup length has the highest value of 8.7 mm for the lowest GLR of 0.55%. By increasing the amount of aeration i.e. increasing GLR, the breakup length reduces to the lower values of 5.9, 4.6, and 1.9 mm for GLRs of 1.1, 1.6, and 2.6%, respectively. The trend of results is in good agreement with those obtained by Tabrizi's [57] experiments as shown in Fig. 3-22.
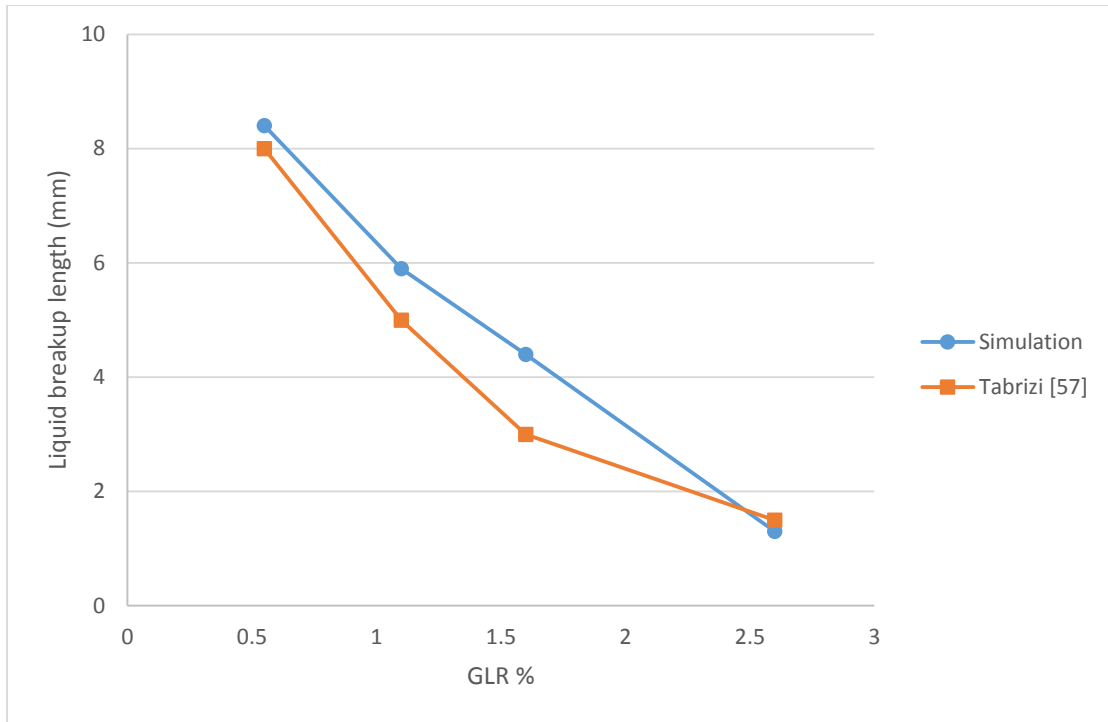
Figure 3-22 Liquid breakup length for different GLRs

The next critical parameter that narrows the application of each atomizer is the cone angle of the spray plum. Fig. 3.23 demonstrates the effect of alternation in GLR on the spray cone angle. These results are obtained by averaging the cone angle through time. As it is obvious in Fig. 3-23, the cone angle increases suddenly from 9.15° to 13.1° due to the transition from the bubbly flow (GLR=0.55%) to the annular flow (GLR=1.1%). By further increase in GLR from 1.1 to 2.6%, the cone angle gradually increases to its maximum value. At the bubbly flow regime, the expansion of the bubbles helps to overcome surface forces. However, in the annular regime, the resultant breakups are due to overcoming aerodynamic forces on the liquid sheets. The trend of growth of the cone angle is in good agreement with the experimental results of Tabrizi [57].

It should be mentioned that altering the liquid properties has a significant effect on the cone angle where the suspension has a wider cone angle in comparison to water. This

60

wider cone angle is due to lower value of surface tension in the suspension, which is because of overcoming of the aerodynamic forces.
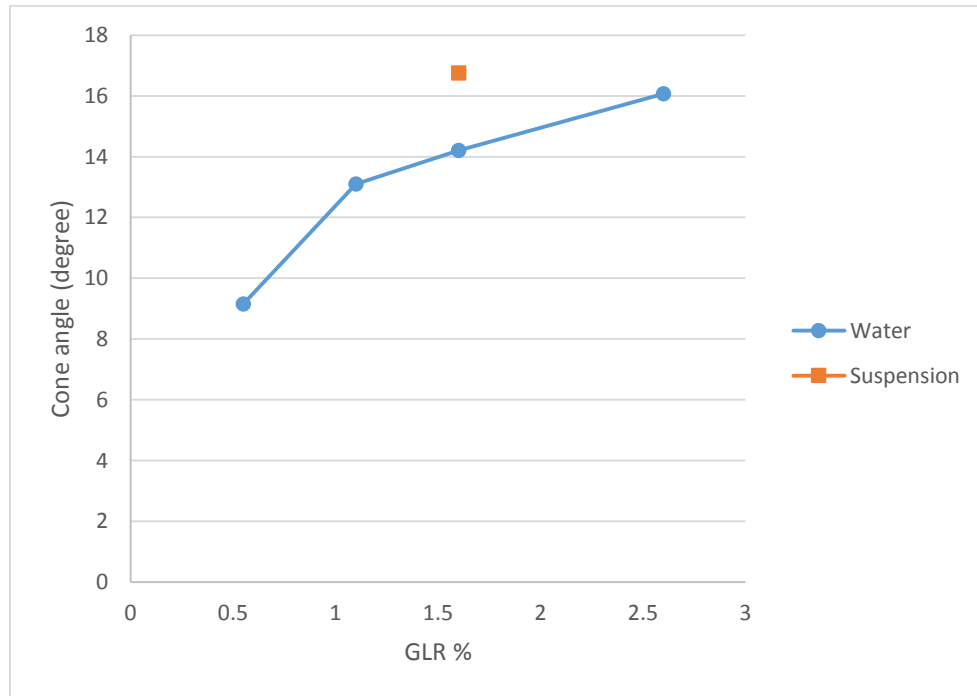
Figure 3-23 Variations of the cone angle for different GLRs and liquid properties

3.2.2 Near-field velocity analysis

A few of the determinant parameters of the atomization is the velocity of liquid and air and their relative velocity defining the downstream characteristics of the droplets. Tabrizi [57] has characterized the velocity profile of the downstream for different GLRs and liquid properties, though he had not characterized near field of the nozzle where the PIV and PDPA are not able to capture the velocity. This inability is due to the existence of the liquid trunk in that region. In this section,

the near field characteristics as well as the effect of liquid properties are comprehensively studied.
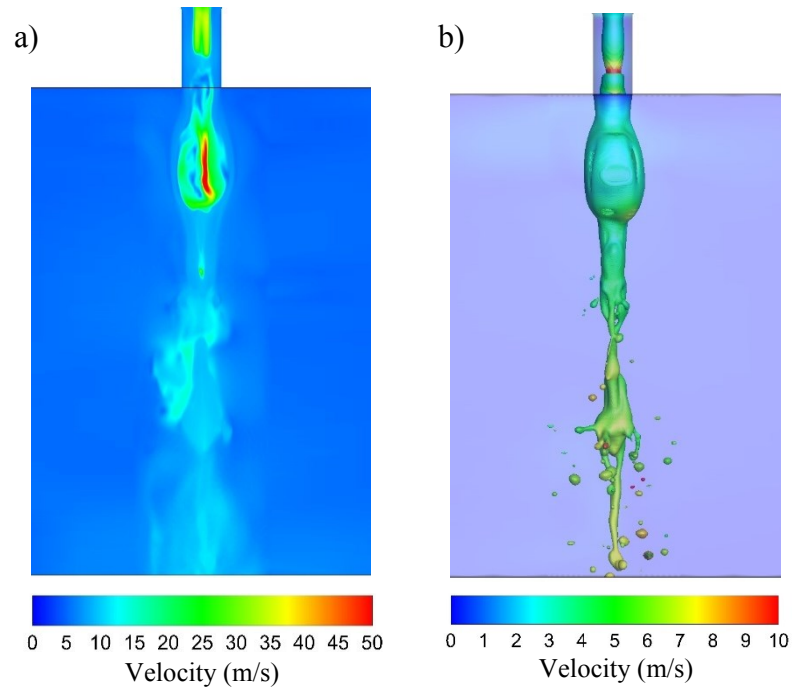
Figure 3-24 Velocity contours of a) air b) liquid in GLR=0.55%
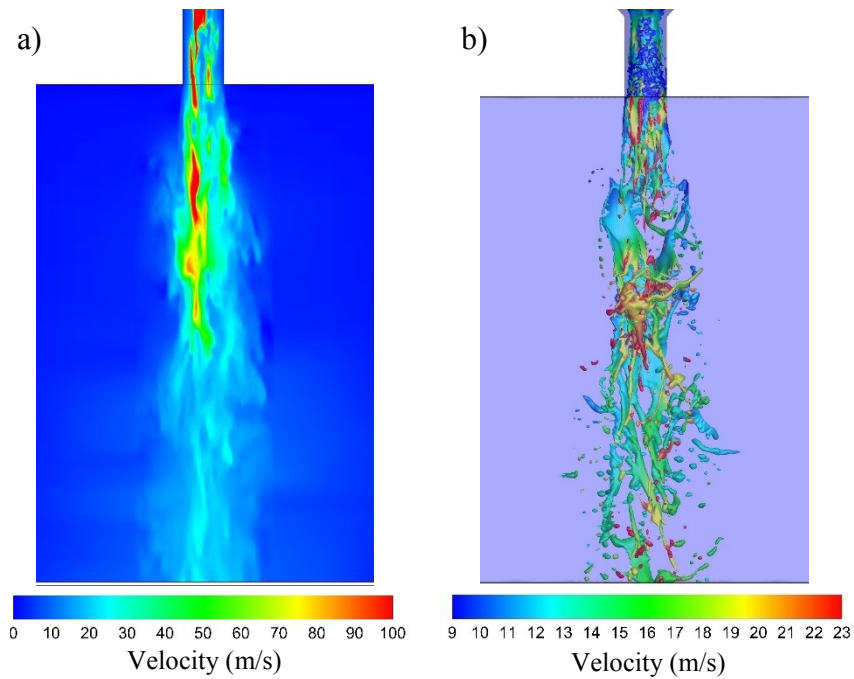
Figure 3-25 Velocity contours of a) air b) liquid for GLR=1.1%
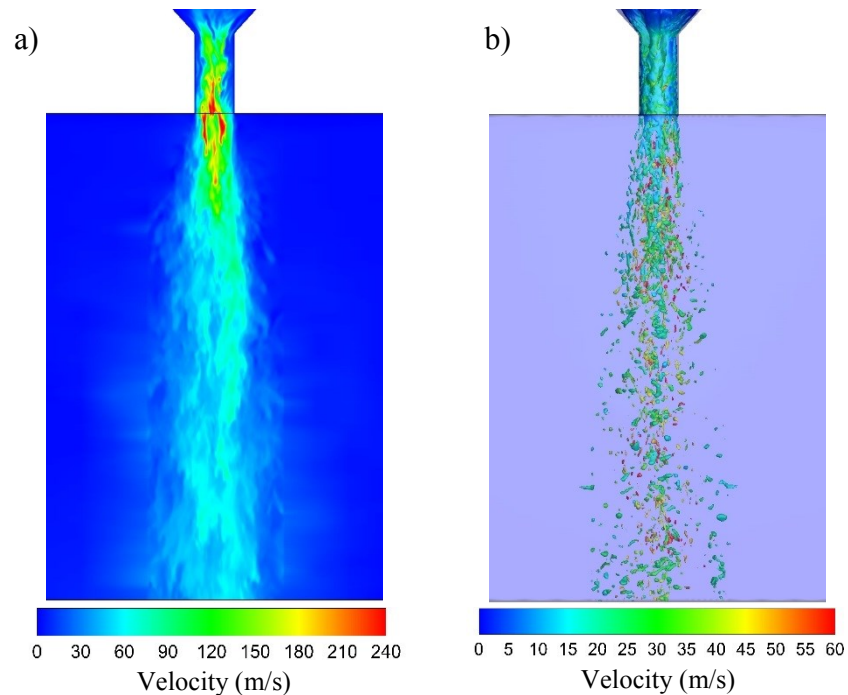
Figure 3-26 Velocity contours of a) air b) liquid for GLR=2.6%

Preliminary, the effect of different GLRs is obvious in Fig. 3-24 to 3-26. At the lowest GLR (0.55%), the velocity of air is at its lowest value with a maximum value of 50 m/s near the nozzle exit and lowest value of 10 m/s at the end of domain. Consequently, the velocity of liquid is in the range of 3-7 m/s. Since the pattern of the atomization in the lower GLR is undesirable for our application, further increase in GLR is required to reach to the applicable range. The results illustrate that by increasing GLR from 0.55 to 1.1%, the velocity of both phases increase to the higher value of 100 m/s for air and 23 m/s for the liquid phase. The average velocity of the liquid for a GLR of 1.1% is around 13 m/s. Additional increase in GLR up to 2.6% leads to significantly higher and wider velocity profile for air phase and consequently the liquid phase. In here, it should be noted that higher velocity in liquid phase for higher GLRs is because of the higher gas velocity and the thinner liquid film thickness discussed in the internal flow section. In the

internal flow, an increase in the gas flow rate squeezes the liquid film thickness, thus the liquid exists from the discharge orifice with the higher velocity.

The significant difference between the velocity of the liquid and the gas phase illustrated in these figures shows the effect of aerodynamic forces on the primary breakup of the liquid trunk. This slip velocity between the liquid and the gas is shown in Fig. 3-27.
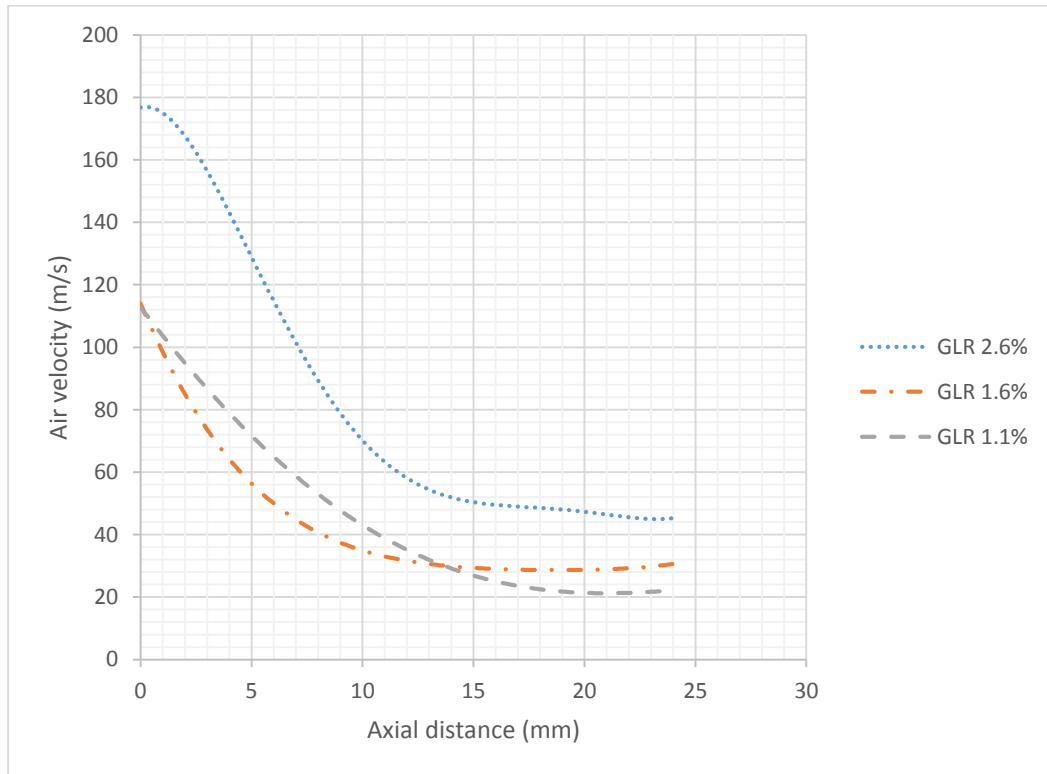
Figure 3-27 The average velocity of air in different axial location and GLRs

As it is depicted in Fig. 3-27, the average velocity of the gas phase at the discharge orifice is at its higher value. Since the energy of the gas phase is low, the velocity of the gas phase reduces by further increase in axial distance from the discharge orifice. This high value of the relative velocity between two phases dominates the aerodynamic forces and produce high shear stress rate at the nozzle exit. These shear stresses along with

surface disturbances start the primary breakup of liquid trunk to ligaments and droplets. This effect is more obvious for the maximum GLR, where the generated droplets are smaller and there is no liquid trunk in downstream of region. The high relative velocity close to the discharge orifice is also reported by Qian et al. [60]. In addition, the momentum energy of the gas phase transferring to the liquid phase helps a better penetration rate for the droplets. Fig 3-28 and 3-29 show the penetration rate of the gas phase and the liquid phase for the largest GLR of 2.6%.
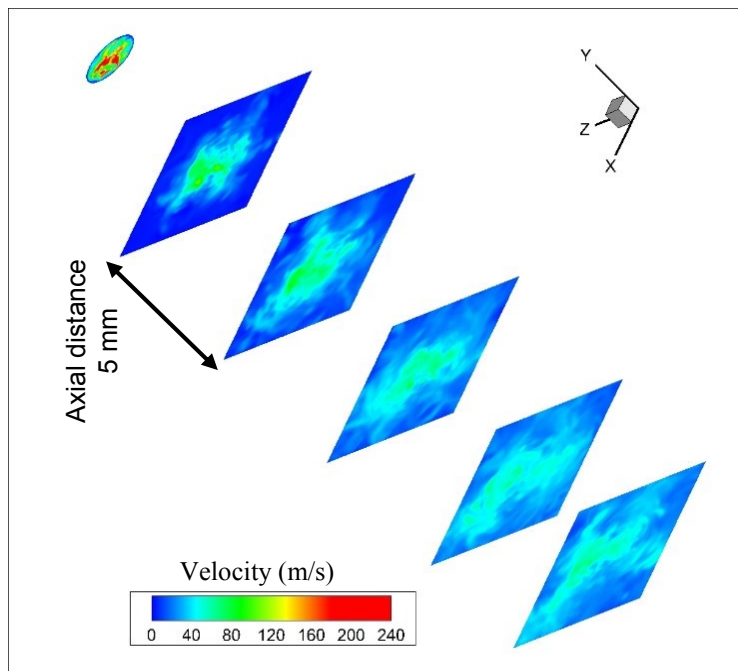
Figure 3-28 The penetration of air for different axial distances of

zero, 5, 10, 15, 20 and 25 mm for GLR=2.6%
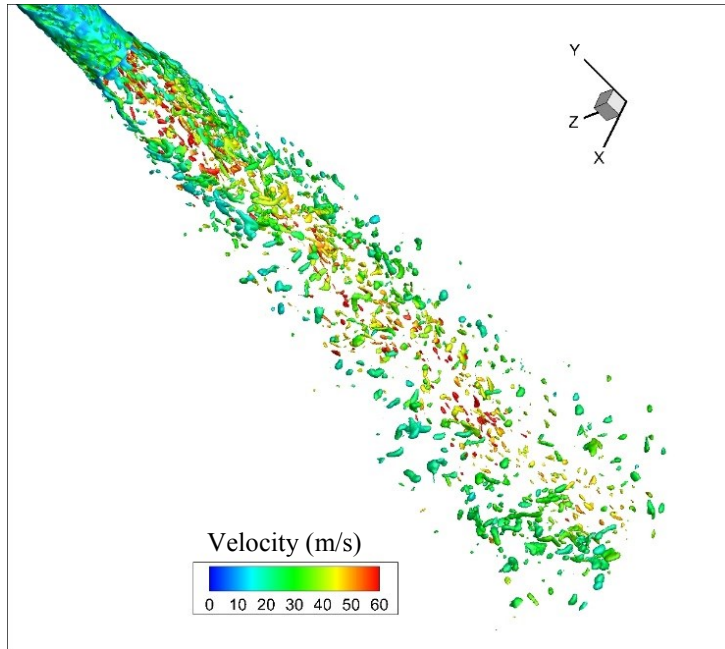
Figure 3-29 The velocity and the pattern of the liquid in different axial distances for GLR=2.6%

At close distances to the nozzle exit, the gas phase velocity is at the maximum and focused in the smaller region. The increase in the axial distance illustrated that the gas phase energy starts to dissipate in the field and reduces by the increase of axial distance. High air momentum transferring to the liquid at the center of profile enhances the velocity of liquid droplets in that region. Consequently, a velocity profile with the higher velocity at the center is obtained.

The other significantly effective parameters on the internal flow are the liquid properties. The comparison between the velocity of the liquid and the gas for the suspension and water is depicted in Fig. 3-30. By closely inspecting the two cases, it is revealed that the gas phase has the higher average velocity with wider dissipation angle. The result of wider dissipation has been seen in the cone angle difference where the suspension case provides a larger cone angle compared to the water case. The penetration of air in the suspension case is higher as well. The liquid droplets and the average

66

velocity in suspension are relatively greater than those of the water case since air and consequently the liquid phase in suspension case have higher momentum. The relative higher velocity for the suspension has been also reported by Tabrizi [57]. The wider cone angle and the higher interface disturbances are due to the smaller surface tension of the suspension. Moreover, the higher momentum of the suspension is because of its higher density. Finally, as it was reported by Tabrizi [57], the liquid properties do not have high influence on the final generated droplet size and their distribution, though this study demonstrate that they change the internal and near field characteristics of the Effervescent nozzle.
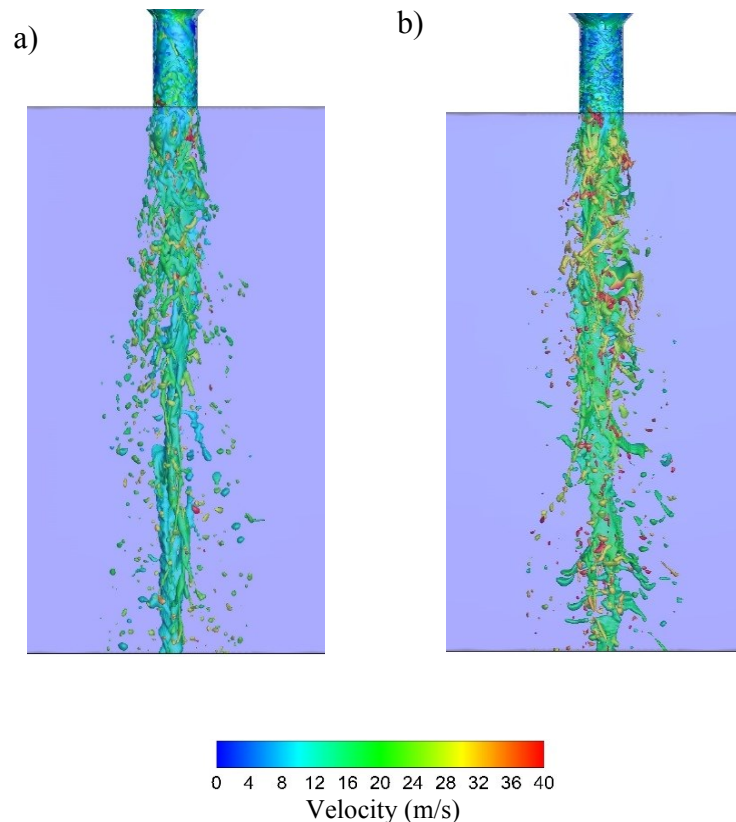

Figure 3-30 Contours of velocity at GLR=1.6% for a) water b) suspension

4 Closure

In this chapter, a summary of the study is outlined. In addition, the conclusions and suggestion for the future works are given.

4.1 Summary of work

In this study, a three dimensional analysis of the two-phase flow inside and outside of an Effervescent nozzle was carried out. For achieving this goal, a compressible, Eulerian two-phase model along with VOF surface capturing method is employed to simulate the internal and the external flow. Moreover, LES turbulence model is used to capture highly turbulent flow. The effect of four different gas to liquid ratios (GLR) on the structure of the internal flow (i.e. flow pattern at the discharge orifice and liquid film thickness) are investigated. Furthermore, thermo physical properties of the liquid and gas phase are locally studied and the effect of critical condition and choked flow inside the nozzle are explained.

In the second part of the results, the influence of these internal structures on the external flow characteristics, such as the cone angle and the breakup length were investigated. The results were compared with the experimental studies of Tabrizi [57] conducted in our lab. Finally, the velocity contour and the slip condition occurring in the near field region of the nozzle were studied in details.

4.2 Conclusion

Employing the surface capturing method in this study helped to capture the internal flow regimes of Effervescent nozzle. The results of numerical study for the internal flow illustrated that for the lowest GLR of 0.55%, the structure of the internal flow is like bubbly flow where the separated bubbles in the discharge orifice passage result in a random bubble bursting. The consequence is having random breakups. By

increasing GLR to 1.1 and 2.6%, the regime changes to the annular flow and the film thickness reduces. The annular flow at the discharge orifice squeezes the liquid to the walls of the nozzle and at the orifice exit, the liquid sheets exit with high oscillation. The enhanced interface disturbances due to higher interaction of the gas/liquid phases lead to faster breakups.

The study of the thermo physical behaviors of the multiphase flow upon exiting from the discharge orifice demonstrates the pressure jump occurring at the nozzle exit and its oscillatory behaviors. These pressure jumps are the consequence of the choking flow even at low velocities since the speed of sound in the multiphase flow reduces to the values of 20-30 m/s. Furthermore, the oscillatory behaviors of pressure in the nozzle illustrate the unsteadiness of the flow Effervescent sprays where it frequently reaches to its critical condition. In addition, the oscillations at the discharge orifice cause the higher amplitude of oscillations in the upstream of the nozzle and particularly in the liquid phase. The alternation of the liquid properties increased the average pressure and oscillation magnitudes in the nozzle, which is due to the lower surface tension of the suspension. However, the damping rate of oscillations for suspension is higher for the liquid phase due to its higher viscosity.

Since the structure of the internal flow governs the external characteristics of the Effervescent nozzle, the longer breakup length and narrower cone angle were obtained for the lowest GLR of 0.55%, where there is a bubbly flow. The annular flow inside the nozzle resulted in shorter breakup length and wider cone angle. The trend of results demonstrated that further increase in GLR leads to shorter breakup length and wider cone angle.

The velocity contours illustrated that the velocity of the liquid and the gas phase in the lower aerating level is in its lowest value and by the increase of GLR, the gas and liquid velocity increases. The higher GLRs showed a greater slip velocity between the two phases and consequently faster breakups with smaller generated droplets. The thinner liquid film thickness affected the external velocity where the thinner the liquid sheet, the higher the outlet velocity. Moreover, the aerating gas helped the liquid droplets to penetrate more into the domain. In addition, the alternation of suspension properties (i.e. viscosity, density, and surface tension) increased the velocity and the momentum of the liquid phase. In addition, a wider dissipation of gas phase in the domain occurred.

Finally, the numerical simulation in this study helped to better understand the fundamental phenomena happening in Effervescent atomization and sprays. The Effervescent nozzle is suitable for suspension thermal spray for several reasons. First, due to its capability to handle various liquids without any significant change in final droplet's size and second for its self-cleaning characteristic, which prevents clogging issue. In addition, this investigation can help us in the control of the atomization process significantly. This leads to better usage of this nozzle in the suspension thermal spray and obtaining more controlled final coating.

4.3   Future works

For more comprehensive understanding of the phenomena occurring in Effervescent nozzle for various applications the following suggestions would be good examples to follow:

- Experimental quantitative study of near-field and discharge passage of effervescent atomization

- Coupling the Volume of fluid method and Level set method for better capturing of the two-phase.

- Coupling the mentioned method with a Lagrangian approach to study the secondary atomization of droplets in downstream of nozzle, which helps to obtain a full comprehensive model.

- Further numerical study on the effect of the liquid and the gas properties on the internal and the external flow.

- Investigating the effect of the cross flow on the atomization and penetration of Effervescent atomization. (Preliminary result for this section were obtained by author)

- Simulating the whole process of thermal spray while using Effervescent injection.

Bibliography

[1]   I. Mamoru and H. Takashi, Thermo-Fluid Dynamics of Two-Phase Flow, Springer, 2011.

[2]   E. by, J. Davis and D. a. Associates, Handbook of Thermal Spray Technology, ASM International, 2004.

[3]   R. Tucker and Jr, "Thermal Spray Coatings, Surface engineering," in *ASM Handbook*, vol. 5, ASM International, 1994, pp. 497-509.

[4]   S. Eidelman and X. Yang, "Three dimensional simulation of HVOF spray deposition of nanoscale," *Nano Structured Materials,* vol. 9, pp. 79-84, 1997.

[5]   A. Killinger, M. Kuhn and R. Gadow, "High-velocity suspension flame spraying (HVSFS), a new approach for spraying nanoparticles with hypersonic speed," *Surface and Coatings Technology,* no. 201, pp. 1922-1929, 2006.

[6]   M. Aghasibeig, M. Mousavi, F. Ben Ettouill, C. Moreau, R. Wuthrich and A. Dolatabadi, "Electrocatalytically Active Nickel-Based Electrode Coatings Formed by Atmospheric and Suspension Plasma Spraying," *Journal of Thermal Spray Technology,* 2013.

[7]   N. Sharifi, F. Ben Ettouil, M. Mousavi, M. Pugh, A. Dolatabadi and C. Moreau, "Superhydrophobicity and Water Repelling Characteristics of Thermally Sprayed Coatings," *Journal of Thermal Spray Technology,* 2013, in press.

[8]   P. Fauchais, G. Montavon, R. Lima and B. Marple, "Engineering a new class of thermal spray nano-based microstructures from agglomerated nanostructured

particles, suspensions and solutions: an invited review," *Journal of Physics and Applied Physics,* no. 44, 2011.

[9]   L. Pawlowski, "Suspension and solution thermal spray coatings," *Surface and Coatings Technology,* no. 203, pp. 2807-2829, 2009.

[10]   J. Fazilleau, C. Delbos, V. Rat, J. Coudert, P. Fauchais and B. Pateyron, "Phenomena Involved in Suspension Plasma Spraying Part 1: Suspension Injection and Behavior," *Plasma Chem. Plasma Process,* no. 26, pp. 371-391, 2006.

[11]   F. Jabbari, M. Jadidi, R. Wuthrich and A. Dolatabadi, "A Numerical Study of Suspension Injection in Plasma Spraying Process," in *International Thermal Spray Conference and Exposition*, Busan, South Korea, 2013.

[12]   "Reiter," [Online]. Available: http://www.reiter-oft.de/index.php?id=89.

[13]   "Niroinc," [Online]. Available: http://www.niroinc.com/technologies/spray_drying_tech.asp.

[14]   A. Lefebvre, Atomization and Sprays, Hemisphere Pub. Corp., 1989.

[15]   A. Lefebvre, X. Wang and C. Martin, "Spray characteristics of aerated-liquid pressure atomizers," *AIAA J Prop Power,* no. 4, p. 293–298, 1988.

[16]   A. Lefebvre, "A novel method of atomization with potential gas turbine application," *Indian Defence Sci J,* no. 38, p. 353–362, 1988.

[17]   X. Wang, J. Chin and A. Lefebvre, "Influence of gas injector geometry on atomization performance of aerated-liquid nozzles," *Int J Turbo Jet Engines,* no. 6, p. 271–280, 1989.

[18]   T. Roesler and A. Lefebvre, "Studies on aerated-liquid atomization," *Int J Turbo Jet Engines,* no. 6, p. 221–230, 1989.

[19]   H. Buckner, P. Sojka and A. Lefebvre, "Effervescent atomization of coal-water slurries," *ASME Publ,* no. 30, p. 105–108, 1990.

[20]   H. Buckner, P. Sojka and A. Lefebvre, "Effervescent atomization of non-Newtonian single phase liquids," in *Proceedings of the Fourth Annual Conference on Atomization and Spray Systems*, Hartford, 1990.

[21]   J. Otahal, J. Fiser and M. Jicha, "Performance of pressure and effervescent atomizers," *Colloquium fluid dynamics,* 2007.

[22]   S. Sovani, P. Sojka and A. Lefebvre, "Effervescent atomization," *Progress in Energy and Combustion Science,* no. 27, p. 483–521, 2001.

[23]   A. Lefebvre, "Some Recent Developments in Twin-Fluid Atomization," *Part. Syst. Charact.,* vol. 13, no. 3, pp. 205-216, 1996.

[24]   C. Marek and L. Cooper.USA Patent 4,189,914, 1980.

[25]   H. Buckner and P. Sojka, "Effervescent atomization of high viscosity fluids. Part 1: Newtonian liquids," *Atomization Sprays,* no. 1, p. 239–252, 1991.

[26]   H. Buckner, P. Sojka and A. Lefebvre, "Aerated atomization of high viscosity Newtonian liquids," in *Proceedings of the Third Annual Conference on Liquid Atomization and Spray Systems*, Irvine, California, 1989.

[27]   J. Chawla, "Atomization of liquids employing the low sonic velocity in liquid/gas mixtures," in *Proceedings of the Third International Conference on Liquid Atomization and Spray Systems*, 1985.

[28] M. Lund, P. Sojka, A. Lefebvre and P. Gosselin, "Effervescent atomization at low mass flow rates. Part 1: the influence of surface tension," *Atomization Sprays,* pp. 77-89, 1993.

[29] J. Sutherland, P. Sojka and M. Plesniak, "Ligament controlled effervescent atomization," *Atomization Sprays,* no. 7, pp. 383-406, 1997.

[30] J. Sutherland, M. Panchagnula, P. Sojka, M. Plesniak and J. Gore, "Effervescent atomization at low air–liquid ratios," in *Proceedings of the Eighth Annual Conference on Liquid Atomization and Spray Systems*, Troy, MI, 1995.

[31] M. Satapathy, S. Sovani, P. Sojka, J. Gore, W. Eckerle and J. Crofts, "The effect of ambient density on the performance of an effervescent atomizer operating in the MPA injection pressure range," in *PROCEEDINGS OF THE INTERNATIONAL CONFERENCE ON LIQUID ATOMIZATION AND SPRAY SYSTEMS*, Bremen, 1998.

[32] M. Liu, Y. Duan, T. Zhang and Y. Xu, "Evaluation of unsteadiness in effervescent sprays by analysis of droplet arrival statistics – The influence of fluids properties and atomizer internal design," *Experimental Thermal and Fluid Science,* no. 35, pp. 190-198, 2011.

[33] M. Lund, C. Jian, P. Sojka, J. Gore and M. Panchagnula, "The influence of atomizing gas molecular weight on low mass flow rate effervescent atomization," *ASME J Fluids Eng.,* 1988.

[34] M. Rahman, M. Balzan, T. Heidrick and B. Fleck, "Effects of the gas phase molecular weight and bubble size on effervescent atomization," *International*

Journal of Multiphase Flow, no. 38, pp. 35-52, 2012.

[35] R. Roesler and A. Lefebvre, "Photographic studies on aeratedliquid atomization, combustion fundamentals and applications," in *Proceedings of the Meeting of the Central States Section of the Combustion Institute*, Indianapolis, Indiana, 1988.

[36] J. Chin and A. Lefebvre, "Flow regimes in effervescent atomization," *Atomization Sprays,* pp. 463-475, 1993.

[37] J. Whitlow and A. Lefebvre, "Effervescent atomizer operation and spray characteristics," *Atomization Sprays,* pp. 137-156, 1993.

[38] P. Santangelo and P. Sojka, "A holographic investigation of the near nozzle structure of an effervescent atomizer produced spray," *Atomization Sprays,* no. 5, pp. 137-155, 1995.

[39] H. Buckner and P. Sojka, "Effervescent atomization of high viscosity fluids, Part 2: Non-Newtonian liquids," *Atomization Sprays,* no. 3, pp. 157-170, 1993.

[40] H. Xiong, J. Lin and Z. Zhu, "Three-dimensional simulation of effervescent atomization spray," *Atomization Sprays,* no. 19, pp. 1-16, 2009.

[41] S. Esfarjani and A. Dolatabadi, "A 3D simulation of two-phase flow in an effervescent atomizer for suspension plasma spray," *Surf Coatings Tech,* no. 203, pp. 2074-2080, 2009.

[42] E. by and N. Ashgriz, Handbook of atomization and sprays theory and applications: Theory and Applications, Springer.

[43] F. Harlow and J. Welsh, "Numerical calculation of time dependent viscous incompressibleflow with a free surface," *Physics of Fluids,* no. 8, pp. 2182-2189,

1965.

[44] C. Hirt and B. Nicholls, "Volume of fluid (VOF) method for the dynamics of free boundaries," *Journal of Computational Physics,* no. 39, pp. 201-225, 1981.

[45] S. Osher and R. Fedkiw, "Level set methods," *Journal of Computational Physics,* no. 169, pp. 463-502, 2001.

[46] D. Anderson, G. McFadden and A. Wheeler, "Diffuse-interface methods in fluid mechanics," *Annual Review of Fluid Mechanics,* no. 30, pp. 139-165, 1998.

[47] J. Glimm, J. Grove, X. Li, K. Shyue, Q. Zhang and Y. Zeng, "Three-dimensional front tracking," *SIAM Journal of Scientific Computing,* no. 19, pp. 703-727, 1998.

[48] G. Tryggvason, B. Bunner, A. Esmaeeli, D. Juric, N. Al-Rawahi, W. Tauber, J. Han, S. Nas and Y. Jan, "A front tracking method for the computations of multiphase flow," *Journal of Computational Physics,* no. 169, pp. 708-759, 2001.

[49] H. Udaykumar, R. Mittal and W. Shyy, "Computation of solid-liquid phase fronts in the sharp interface limit on fixed grids," *Journal of Computational Physics,* no. 153, pp. 535-574, 1999.

[50] M. Francois and W. Shyy, "Computations of drop dynamics with the immersed boundary method, part 1: numerical algorithm and buoyancy-induced effect," *Numerical Heat Transfer,* no. 44, pp. 101-118, 2003.

[51] L. Lee and R. Leveque, "An immersed interface method for incompressible Navier-Stokes equations," *SIAM Journal of Scientific Computing,* no. 25, pp. 832-856, 2003.

[52] M. Van Sint Annaland, N. Deen and J. Kuipers, "Numerical simulation of gas

bubbles behaviour using a three-dimensional volume of fluid method," *Chemical Engineering Science,* no. 60, pp. 2999-3011, 2005.

[53] "OpenCFD Ltd.," [Online]. Available: http://www.openfoam.org/.

[54] H. Rusche, "Computational fluid dynamics of dispersed two-phase flows at high phase fractions," Dpt. of Mech. Eng., Imperial College, London, 2002.

[55] A. Yoshizawa and K. Horiuti, "A Statistically-Derived Sub-Grid Scale Model for the Large Eddy Simulation of Turbulent Flows," *J. Phys. Soc. Jpn.,* no. 54, pp. 2834-2839, 1985.

[56] "Compute Canada," [Online]. Available: https://computecanada.ca.

[57] H. Farshchi Tabrizi, "Experimental study of Effervescent atomization," Concordia university, Montrea, Canada, 2013.

[58] K. Lin, P. Kennedy and T. Jackson, "Structures of Internal Flow and the Corresponding Spray for Aerated-Liquid Injectors," *AIAA,* 2001.

[59] S. Churchill and R. Usagi, "A general expression of the correlation of rates of transfer and other phenomena," *AIChE Journal,* vol. 6, no. 18, pp. 1121-1128, 1972.

[60] L. Qian, J. Lin, H. Xiong and e. al, "Theoretical investigation of the influence of liquid physical properties on effervescent atomization performance," *ASME J Fluids Eng,* p. 133, 2011.